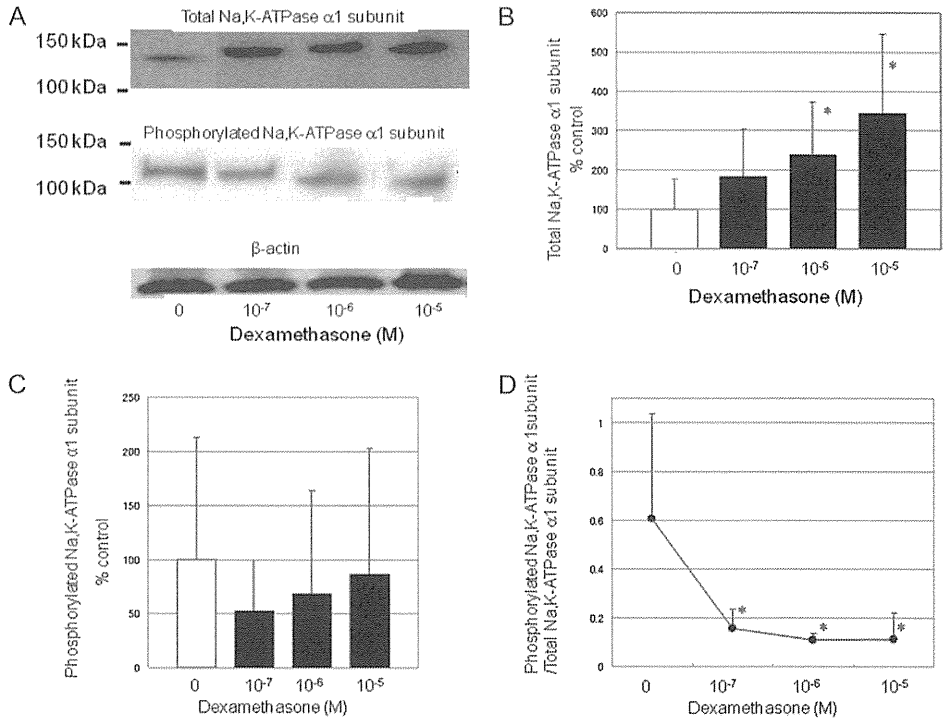

FIGURE 4. Western blot analysis of Na,K-ATPase α_1-subunit and phospho-Na,K-ATPase α_1-subunit expression. A, Representative signals of expression. Top: Na,K-ATPase α_1-subunit. Middle: phospho-Na,K-ATPase α_1-subunit. Bottom: β-actin. The relative intensity of each band with respect to β-actin was measured and expressed as a ratio. B, Cells were incubated with the indicated concentrations of dexamethasone for 48 hours and then assayed for expression of the Na,K-ATPase α_1-subunit. Data are means ± SDs from 5 experiments, expressed as a percentage of control. $^*P < 0.05$ for the indicated comparisons (Student *t* test). C, Cells were incubated with the indicated concentrations of dexamethasone for 48 hours and then assayed for expression of the phospho-Na,K-ATPase α_1-subunit. Data are means ± SDs from 5 experiments, expressed as a percentage of control. D, The rate of the inactive state of Na,K-ATPase α_1-subunit with the indicated concentrations of dexamethasone. The values represent the ratio of phospho-Na,K-ATPase α_1-subunit expression to Na,K-ATPase α_1-subunit expression. Data are means ± SDs of values from 5 experiments. $^*P < 0.05$ for the indicated comparisons (Student *t* test). Modified with permission from Hatou et al.[32]

In the presence of staurosporine, GF109203X, and okadaic acid, the expression of total Na,K-ATPase α_1-subunit was unchanged; however, insulin-induced dephosphorylation of the Na,K-ATPase α_1-subunit was diminished.

Immunocytochemistry was employed to determine whether the effects of insulin changed cell surface expression of the Na,K-ATPase α_1-subunit. Insulin-treated corneal endothelial cells expressed more Na,K-ATPase α_1-subunit at their lateral cell membranes compared with control cells. In the presence of inhibitors, such as GF109203X, Na,K-ATPase α_1-subunit expression at the lateral cell membrane was observed to be decreased (Fig. 9A–C).[33]

DISCUSSION

We have shown that dexamethasone increases Na,K-ATPase activity and pump function in cultured corneal endothelial cells. Changes in Na,K-ATPase activity and pump function were strongly correlated under various experimental conditions. Our results support the stimulatory effect of dexamethasone on Na,K-ATPase activity in corneal endothelial cells.

Our results further suggest that the regulation of Na,K-ATPase activity by dexamethasone in corneal endothelial cells was mediated by Na,K-ATPase subunit synthesis. Na,K-ATPase is the largest protein complex in the family of P-type cation pumps, and its minimum functional unit is a heterodimer of the α- and β-subunits.[34] Ewart and Klip[8] reported that the activation of Na,K-ATPase by steroid hormones seemed to be mediated by the synthesis of new α- and β-subunits. In our study, dexamethasone increased the proportion of active-state Na,K-ATPase α_1-subunits and the total number of Na,K-ATPase α_1-subunits. The antiphospho-Na/K-ATPase α_1 antibody we used recognizes the Na,K-ATPase α_1-subunit only when phosphorylated at Ser-18. Phosphorylation at Ser-18 triggers endocytosis of Na,K-ATPase α_1-subunits and results in inhibition of Na,K-ATPase activity.[35,36] Dexamethasone may prevent Na,K-ATPase α_1-subunits from Ser-18 phosphorylation and thereby increase the proportion of active-state Na,K-ATPase α_1-subunits.

Our results showed that insulin increased Na,K-ATPase activity and pump function in cultured corneal endothelial cells, but the observed effect of insulin on Na,K-ATPase activity was transient. A lack of insulin in type 1 diabetes mellitus or a chronic reduced level of insulin signaling because of insulin resistance in type 2 diabetes mellitus is essential for the pathogenesis of corneal abnormalities in diabetes.

Insulin has been shown to stimulate electrogenic sodium transport in a variety of cells.[8,37–46] In most cases, the increase in Na^+ transport is thought to be a result of the stimulation of Na,K-ATPase. There have been various advocated mechanisms of insulin action, including changes in the kinetic properties of the enzyme,[37,38] an increase in the intracellular Na^+ concentration that leads to subsequent pump stimulation,[39–43] and an increase in the pump concentration at the cell surface by serum- and glucocorticoid-dependent kinase.[44–46] Regardless of whether insulin stimulates pump activity by a previous increase in cytosolic Na^+, its affinity for Na^+, or in-pump availability at the cell surface, the insulin receptor

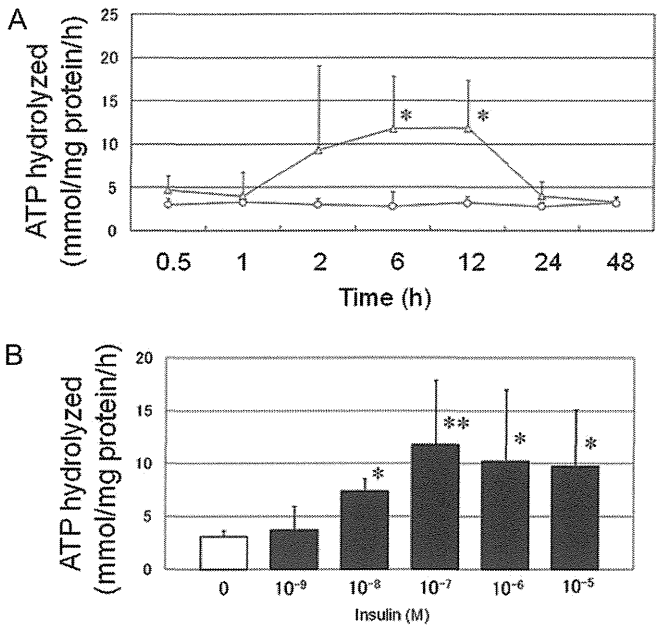

FIGURE 5. Effect of insulin on Na,K-ATPase activity in cultured mouse corneal endothelial cells. A, Cells were incubated in the absence (circles) or presence (triangles) of 0.1 μM insulin for the indicated times and then assayed for Na,K-ATPase activity. Data are means ± SDs of values from 4 replicate experiments. $*P < 0.05$ versus the corresponding value for cells incubated without insulin (Student *t* test). B, Cells were incubated with the indicated concentrations of insulin for 6 hours and then assayed for Na,K-ATPase activity. Data are means ± SDs of values from 4 replicates of 4 representative experiments. $*P < 0.05$, $**P < 0.01$ for the indicated comparisons (Student *t* test). Modified with permission from Hatou et al.[33]

signaling cascades must be involved.[8] These signaling cascades include those mediated by protein kinases, such as PKC. PKC is thought to trigger the rapid action of insulin on Na,K-ATPase and to be involved in the stimulation of Na,K-ATPase by insulin in muscle cells.[8] In our study, Western blot analysis suggested that the stimulation of Na,K-ATPase activity by insulin in corneal endothelial cells was associated with a decrease in the levels of the inactive state of the Na,K-ATPase α_1-subunit. Na,K-ATPase activation by insulin seemed to be mediated by PKC, protein phosphatase 1 (PP1), and/or PP2A. The immunocytochemistry results indicated that insulin increased cell surface expression of the Na,K-ATPase α_1-subunit, and the presence of inhibitors, such as GF109203X, decreased its expression.

In conclusion, we have shown that dexamethasone and insulin increase Na,K-ATPase activity and pump function in corneal endothelial cells. Furthermore, our results support a model in which Na,K-ATPase activation by dexamethasone is mediated by Na,K-ATPase subunit synthesis and an increase in the proportion of Na,K-ATPase α_1-subunits in the active state. In contrast, the observed effect of insulin on Na,K-ATPase activity was transient. This may be because Na,K-ATPase activation by insulin in corneal endothelial cells was mediated by an increase in the active state of the Na,K-ATPase α_1-subunits via PKC, PP1, and/or PP2A pathways, but not by Na,K-ATPase subunit synthesis. A lack of insulin in type 1 diabetes mellitus or a reduced level of insulin signaling caused by insulin resistance in type 2 diabetes mellitus may play a role in the pathogenesis of corneal abnormalities in diabetes. Pharmacological manipulation of dexamethasone or insulin in corneal endothelial cells is a potential therapeutic approach for increasing the pump function in corneal endothelial cells.

REFERENCES

1. Nishida T. Cornea. In: Krachmer JH, Mannis MJ, Holland EJ, eds. *Cornea*. 2nd ed. London, United Kingdom: Elsevier Mosby; 2005:3–26.
2. Feiz V. Corneal edema. In: Krachmer JH, Mannis MJ, Holland EJ, eds. *Cornea*. 2nd ed. London, United Kingdom: Elsevier Mosby; 2005: 359–363.
3. Kang PC, Klintworth GK, Kim T, et al. Trends in the indications for penetrating keratoplasty, 1980–2001. *Cornea*. 2005;24:801–803.
4. Al-Yousuf N, Mavrikakis E, Daya SM. Penetrating keratoplasty: indications over 10 year period. *Br J Ophthalmol*. 2004;88:998–1001.
5. Dobbins KR, Price FW Jr, Whitson WE. Trends in the indications for penetrating keratoplasty in the Midwestern United States. *Cornea*. 2000; 19:813–816.

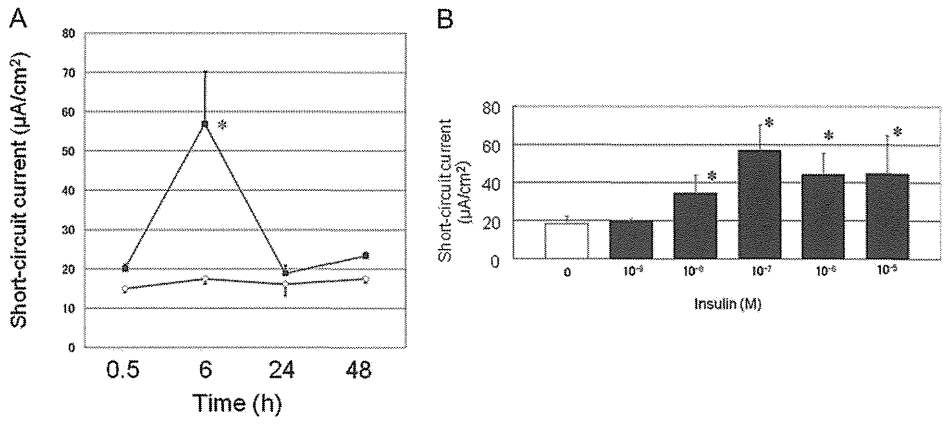

FIGURE 6. Effect of insulin on the pump function of cultured mouse corneal endothelial cells. A, Pump function (microamperes per square centimeter) attributable to Na,K-ATPase activity was determined in the absence (circles) or presence (squares) of 0.1 μM insulin for the indicated times. Data are means ± SDs of values from 4 replicates of a representative experiment. $*P < 0.05$ versus the corresponding value for cells incubated without insulin (Student *t* test). B, Pump function (microamperes per square centimeter) attributable to Na,K-ATPase activity was determined 6 hours after incubation of cells in the presence of the indicated concentrations of insulin. Data are means ± SDs of values from 4 replicates of 4 representative experiments. $*P < 0.05$ for the indicated comparisons (Student *t* test). Modified with permission from Hatou et al.[33]

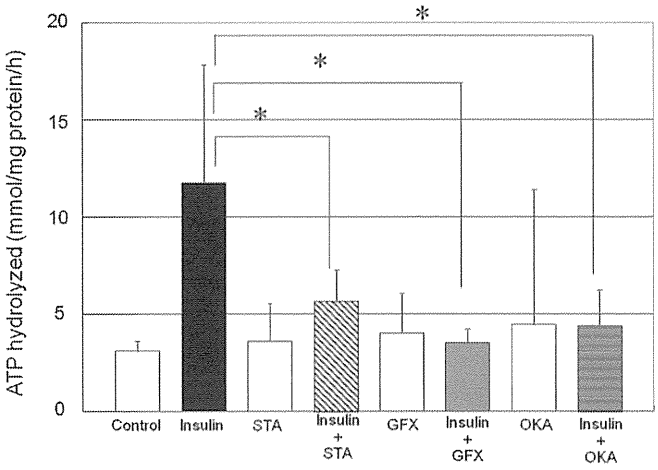

FIGURE 7. Effect of staurosporine (STA), GF109203X (GFX), and okadaic acid (OKA) on insulin-induced Na,K-ATPase activity in cultured mouse corneal endothelial cells. Cells were incubated for 30 minutes in the absence or presence of 1 μM staurosporine, 0.1 μM GF109203X, or 1 μM okadaic acid and then for an additional 6 hours in the presence of 0.1 μM insulin before measurement of Na,K-ATPase activity. Data are means ± SDs of values from 4 replicates of 4 representative experiments. $*P < 0.01$ versus the value for cells incubated with insulin alone (Student *t* test). Na,K-ATPase activity did not significantly increase in the presence of staurosporine + insulin, GF109203X + insulin, or okadaic acid + insulin compared with controls. Modified with permission from Hatou et al.[33]

6. Georski D, Matsuda M, Yee RW, et al. Pump function of the human corneal endothelium. Effects of age and cornea guttata. *Ophthalmology.* 1985;92:759–763.
7. McCartney MD, Wood TO, McLaughlin BJ. Moderate Fuchs' endothelial dystrophy ATPase pump site density. *Invest Ophthalmol Vis Sci.* 1989;30: 1560–1564.
8. Ewart NS, Klip A. Hormonal regulation of the Na^+,K^+-ATPase: mechanisms underlying rapid and sustained changes in pump activity. *Am J Physiol.* 1995;269:C295–C311.
9. Sanchez RO, Polack FM. Effect of topical steroids on the healing of corneal endothelium. *Invest Ophthalmol Vis Sci.* 1974;13:17–22.
10. Chung JH, Paek S, Choi JJ, et al. Effect of topically applied 0.1% dexamethasone on endothelial healing and aqueous composition during the repair process of rabbit corneal alkali wounds. *Curr Eye Res.* 1999;18: 110–116.
11. Olsen E, Dacanger M. The effect of steroids on the healing of the corneal endothelium. An in vivo and in vitro study in rabbits. *Acta Ophthalmol Scand.* 1984;62:893–899.
12. Fukuda K, Takeuchi H, Nishida T. A case of noninflammatory corneal edema following anterior-posterior radial keratotomy (Sato's operation) successfully treated by topical corticosteroid. *Jpn J Ophthalmol.* 2000;44: 520–523.
13. Brightbill FS, Meyers FL, Brensnick GH. Post-vitrectomy keratopathy. *Am J Ophthalmol.* 1978;85:651–655.
14. Foulks GN, Thoft RA, Perry HD, et al. Factors related to corneal epithelial complications after closed vitrectomy in diabetics. *Arch Ophthalmol.* 1979;97:1076–1079.
15. Perry HD, Foulks GN, Thoft RA, et al. Corneal complications after closed vitrectomy through the pars plana. *Arch Ophthalmol.* 1980;96:1401–1403.
16. Mandelcorm MS, Blankenship G, Machemer R. Pars plana vitrectomy for the management of severe diabetic retinopathy. *Am J Ophthalmol.* 1976; 81:561–570.
17. Schultz RO, Van Horn D, Peters MA, et al. Diabetic keratopathy. *Trans Am Ophthalmol Soc.* 1981;79:180–198.

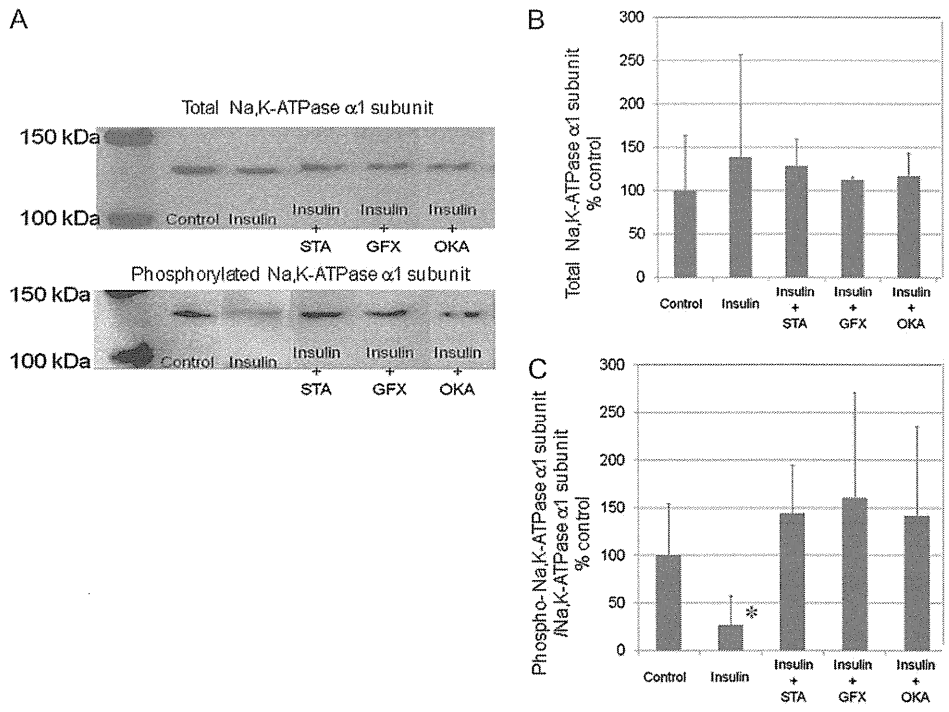

FIGURE 8. Western blot analysis of Na,K-ATPase α_1-subunit and phospho-Na,K-ATPase α_1-subunit expression. A, Representative signals of expression. Top: Na,K-ATPase α_1-subunit. Bottom: phospho-Na,K-ATPase α_1-subunit. The relative intensity of each band compared with β-actin was measured by a densitometer and expressed as a ratio. B, Cells were incubated in the absence (control) or presence of 0.1 μM insulin for 6 hours, 0.1 μM insulin for 6 hours with a 30-minute preincubation with 1 μM staurosporine (insulin + STA), 0.1 μM GF109203X (insulin + GFX), or 1 μM okadaic acid (insulin + OKA) and then assayed for the expression of Na,K-ATPase α_1-subunit. Data are means ± SDs from 5 experiments, expressed as a percentage of control. C, The rate of inactive state of Na,K-ATPase α_1-subunit with insulin, insulin + STA, insulin + GFX, and insulin + OKA. The values represent the ratio of phospho-Na,K-ATPase α_1-subunit expression to Na,K-ATPase α_1-subunit expression. Data are means ± SDs of values from 5 experiments. $*P < 0.05$ versus the value for cells incubated without insulin (Student *t* test). Modified with permission from Hatou et al.[33]

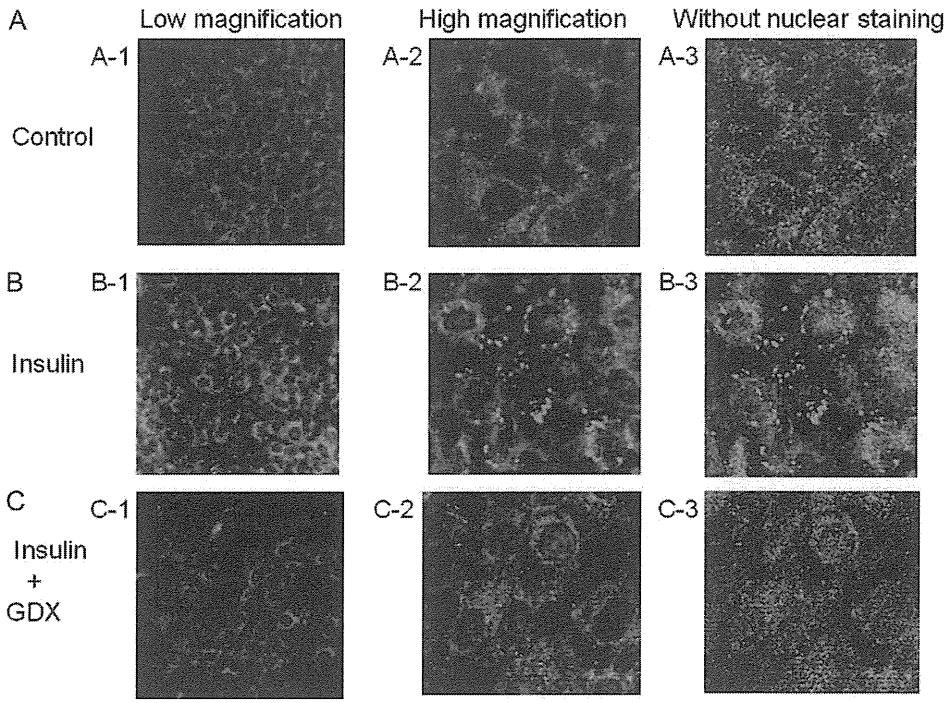

FIGURE 9. Effect of insulin on Na,K-ATPase α_1-subunit cell surface expression. Cells were incubated in the absence of insulin (A) or in the presence of 0.1 μM insulin for 6 hours (B) or 0.1 μM insulin for 6 hours with a 30-minute preincubation with 1 μM GF109203X (C) and then assayed for cell surface expression of the Na,K-ATPase α_1-subunit by immunocytochemistry. A-1, B-1, and C-1: low magnification; A-2, B-2, and C-2: high magnification; and A-3, B-3, and C-3: without nuclear staining. Modified with permission from Hatou et al.[33]

18. Rao GN, Aquavella JV, Goldberg SH, et al. Pseudophakic bullous keratopathy: relationships to preoperative endothelial status. *Ophthalmology.* 1984;91:1135–1140.
19. Rao GN, Shaw EL, Arther EJ, et al. Endothelial cell morphology and corneal deturgescence. *Ann Ophthalmol.* 1978;11:885–899.
20. O'Niel MR, Polse KA. Decreased endothelial pump function with aging. *Invest Ophthalmol Vis Sci.* 1986;27:457–463.
21. Schultz RO, Matsuda M, Yee RW, et al. Corneal endothelial changes in type 1 and type 2 diabetes mellitus. *Am J Ophthalmol.* 1984;98:401–410.
22. Kim EK, Geroski DH, Holley GP, et al. Corneal endothelial cytoskeletal changes in F-actin with aging, diabetes, and after cytochalasin exposure. *Am J Ophthalmol.* 1992;114:331–335.
23. Roszkowska AM, Tringali CG, Colosi P, et al. Corneal endothelium evaluation in type 1 and type 2 diabetes mellitus. *Ophthalmologica.* 1999; 213:258–261.
24. Inoue K, Kato S, Inoue Y, et al. Corneal endothelium and thickness in type 2 diabetes mellitus. *Jpn J Ophthalmol.* 2002;46:65–69.
25. Take G, Karabay G, Erdogan D, et al. The ultrastructural alterations in rat corneas with experimentally-induced diabetes mellitus. *Saudi Med J.* 2006;27:1650–1655.
26. Busted N, Olsen T, Schmitz O. Clinical observations on the corneal thickness and the corneal endothelium in diabetes mellitus. *Br J Ophthalmol.* 1981;65:687–690.
27. Olsen T, Busted N. Corneal thickness in eyes with diabetic and nondiabetic neovascularisation. *Br J Ophthalmol.* 1981;65:691–693.
28. Weston BC, Bourne WM, Polse KA, et al. Corneal hydration control in diabetes mellitus. *Invest Ophthalmol Vis Sci.* 1995;36:586–595.
29. Pierro L, Brancato R, Zaganelli E. Correlation of corneal thickness with blood glucose control in diabetes mellitus. *Acta Ophthalmol (Copenh).* 1993;71:169–172.
30. Skaff A, Cullen AP, Doughty MJ, et al. Corneal swelling and recovery following wear of thick hydrogel contact lenses in insulin-dependent diabetics. *Ophthalmol Physiol Opt.* 1995;15:287–297.
31. Saini JS, Mittal S. In vivo assessment of corneal endothelial function in diabetes mellitus. *Arch Ophthalmol.* 1996;114:649–653.
32. Hatou S, Yamada M, Mochizuki H, et al. The effects of dexamethasone on the Na,K-ATPase activity and pump function of corneal endothelial cells. *Curr Eye Res.* 2009;34:347–354.
33. Hatou S, Yamada M, Akune Y, et al. Role of insulin in regulation of Na+-/K+-dependent ATPase activity and pump function in corneal endothelial cells. *Invest Ophthalmol Vis Sci.* 2010;51:3935–3942.
34. Jorgensen PL, Hakansson KO, Karlish SJ. Structure and mechanism of Na,K-ATPase: functional sites and their interactions. *Annu Rev Physiol.* 2003;65:817–849.
35. Chibalin AV, Ogimoto G, Pedemonte CH, et al. Dopamine-induced endocytosis of Na+,K+-ATPase is initiated by phosphorylation of Ser-18 in the rat alpha subunit and is responsible for the decreased activity in epithelial cells. *J Biol Chem.* 1999;274:1920–1927.
36. Yudowski GA, Efendiev R, Pedemonte CH, et al. Phosphoinositide-3 kinase binds to a proline-rich motif in the Na+, K+-ATPase alpha subunit and regulates its trafficking. *Proc Natl Acad Sci U S A.* 2000;97:6556–6561.
37. Feraille E, Carranza ML, Rousselot M, et al. Insulin enhances sodium sensitivity of Na-K-ATPase in isolated rat proximal convoluted tubule. *Am J Physiol.* 1994;267(pt2):F55–F62.
38. Deachapunya C, Palmer-Densmore M, O'Grady SM. Insulin stimulates transepithelial sodium transport by activation of a protein phosphatase that increases Na-K ATPase activity in endometrial epithelial cells. *J Gen Physiol.* 1999;114:561–574.
39. Siegel B, Civan MM. Aldosterone and insulin effects on driving force of Na^+ pump in toad bladder. *Am J Physiol.* 1976;230:1603–1608.
40. Walker TC, Fidelman ML, Watlington CO, et al. Insulin decreases apical membrane resistance in cultured kidney cells (A6). *Biochem Biophys Res Commun.* 1984;124:614–618.
41. Blazer-Yost BL, Cox M, Furlanetto J. Insulin and IGF-I receptor-mediated Na^+ transport in toad urinary bladders. *Am J Physiol.* 1989;257:C612–C620.
42. McGill DL, Guidotti G. Insulin stimulates both the alpha 1 and the alpha 2 isoforms of the rat adipocyte (Na+,K+) ATPase. Two mechanisms of stimulation. *J Biol Chem.* 1991;266:15824–15831.
43. Erlij D, De Smet P, Van Driessche W. Effect of insulin on area and Na^+ channel density of apical membrane of cultured toad kidney cells. *J Physiol.* 1994;481:533–542.
44. Henke G, Setiawan I, Bohmer C, et al. Activation of Na^+/K^+-ATPase by the serum and glucocorticoid-dependent kinase isoforms. *Kidney Blood Press.* 2002;25:370–374.
45. Park J, Leong ML, Buse P, et al. Serum and glucocorticoid-inducible kinase (SGK) is a target of the PI 3-kinase-stimulated signaling pathway. *EMBO J.* 1999;18:3024–3033.
46. Verry F, Summa V, Heitzmann D, et al. Short-term aldosterone action on Na,K-ATPase surface expression: role of aldosterone-induced SGK1? *Ann N Y Acad Sci.* 2003;986:554–561.

Establishment of Functioning Human Corneal Endothelial Cell Line with High Growth Potential

Tadashi Yokoi[1,2], Yuko Seko[1,7], Tae Yokoi[1], Hatsune Makino[3], Shin Hatou[4], Masakazu Yamada[5], Tohru Kiyono[6], Akihiro Umezawa[3], Hiroshi Nishina[2], Noriyuki Azuma[1]*

1 Department of Ophthalomology, National Center for Child Health and Development, Tokyo, Japan, **2** Department of Developmental and Regenerative Biology, Medical Research Institute, Tokyo Medical and Dental University, Bunkyo-ku Tokyo, Japan, **3** Department of Reproductive Biology, National Research Institute for Child Health and Development, Tokyo, Japan, **4** Department of Ophthalmology, Keio University School of Medicine, Tokyo, Japan, **5** Division for Vision Research, National Institute of Sensory Organs, National Tokyo Medical Center, Tokyo, Japan, **6** Division of Virology, National Cancer Center Research Institute, Tokyo, Japan, **7** Sensory Functions Section, Research Institute, National Rehabilitation Center for Persons with Disabilities, Tokyo, Japan

Abstract

Hexagonal-shaped human corneal endothelial cells (HCEC) form a monolayer by adhering tightly through their intercellular adhesion molecules. Located at the posterior corneal surface, they maintain corneal translucency by dehydrating the corneal stroma, mainly through the Na^+- and K^+-dependent ATPase (Na^+/K^+-ATPase). Because HCEC proliferative activity is low *in vivo*, once HCEC are damaged and their numbers decrease, the cornea begins to show opacity due to overhydration, resulting in loss of vision. HCEC cell cycle arrest occurs at the G1 phase and is partly regulated by cyclin-dependent kinase inhibitors (CKIs) in the Rb pathway (p16-CDK4/CyclinD1-pRb). In this study, we tried to activate proliferation of HCEC by inhibiting CKIs. Retroviral transduction was used to generate two new HCEC lines: transduced human corneal endothelial cell by human papillomavirus type E6/E7 (THCEC (E6/E7)) and transduced human corneal endothelial cell by Cdk4R24C/CyclinD1 (THCEH (Cyclin)). Reverse transcriptase polymerase chain reaction analysis of gene expression revealed little difference between THCEC (E6/E7), THCEH (Cyclin) and non-transduced HCEC, but cell cycle-related genes were up-regulated in THCEC (E6/E7) and THCEH (Cyclin). THCEH (Cyclin) expressed intercellular molecules including ZO-1 and N-cadherin and showed similar Na^+/K^+-ATPase pump function to HCEC, which was not demonstrated in THCEC (E6/E7). This study shows that HCEC cell cycle activation can be achieved by inhibiting CKIs even while maintaining critical pump function and morphology.

Citation: Yokoi T, Seko Y, Yokoi T, Makino H, Hatou S, et al. (2012) Establishment of Functioning Human Corneal Endothelial Cell Line with High Growth Potential. PLoS ONE 7(1): e29677. doi:10.1371/journal.pone.0029677

Editor: Irina Kerkis, Instituto Butantan, Brazil

Received July 18, 2011; **Accepted** December 2, 2011; **Published** January 19, 2012

Funding: This study was supported by a grant (#18390473) from the Ministry of Education, Culture, Sports, Science and Technology (MEXT) of Japan. The funders had no role in study design, data collection and analysis, decision to publish, or preparation of the manuscript.

Competing Interests: The authors have declared that no competing interests exist.

* E-mail: azuma-n@ncchd.go.jp

Introduction

Human corneal endothelial cells (HCEC) are hexagonal in shape and form a fragile monolayer lying posterior to the surface of the cornea. These cells maintain corneal transparency by their tight intercellular barrier and perform an ion transport pump function through Na^+/K^+-ATPase, which regulates the hydration of the corneal stroma [1,2]. If HCEC sustain damage, excessive hydration and opacity of the cornea occur, resulting in decreased vision.

Corneal endothelia are believed not to increase in adult humans and in fact gradually decrease by approximately 0.5% per year [3,4,5]. Damage, injury or HCEC disease such as Fuchs' corneal dystrophy [6], diabetes [7], trauma [8], cataract surgery [9] or elevation of intraocular pressure [10] does not lead to increased proliferation but rather to an increase in cell size to compensate for the wounded area [11]. Once the cell number falls below 1,000 cells/mm^2, the monolayer of enlarged HCEC cannot maintain corneal translucency [12] and surgical treatment is required to restore vision.

Penetrating keratoplasty has long been the surgical treatment of choice, involving replacement of a total layer of cornea by donor material. However, it can also result in adverse effects such as astigmatism and severe rejection requiring long term usage of immunosuppressive drugs [13]. Recently, alternative transplantation strategies, including modified posterior lamellar keratoplasty techniques such as deep lamellar endothelial keratoplasty (DLEK) [14], Descemet's stripping with endothelial keratoplasty (DSEK) [15] and Descemet membrane endothelial keratoplasty (DMEK) [16] have been introduced to overcome these problems. Despite these advances, an increasingly aging population requiring corneal transplants and inadequate tissue quality limit the availability of donor corneas, such that alternative ways of preparing endothelial cell monolayers need to be explored.

HCEC were originally believed to be incapable of expanding *in vitro*, but have been successfully isolated and cultured by introducing stimulating agents such as epidermal growth factor, platelet-derived growth factor-BB, bovine pituitary extract and fetal bovine serum [17,18]. However, the number of cells with proliferative activity and the ability to respond to such agents is relatively low, and much variation in proliferative activity exists between donors of different ages [19,20]. Thus, there is a requirement to achieve a stable and effective culture of cells in terms of both cell proliferation and physiologic function.

The HCEC cell cycle is mainly regulated by the p53 and pRB pathways, both of which have been inactivated by human papilloma virus (HPV) type 16 E6/E7 to successfully immortalize cells. Kim et al. reported the establishment of an immortalized HCEC line using HPV type 16 E6/E7 on lyophilized human amniotic membrane [21]. However, several studies have reported carcinogenesis of the cell line established by viral oncogenes including HPV type 16 E6/E7 or SV40 large T antigen [22,23]. Therefore a corneal endothelial cell line developed in this way does not appear to be suitable for the treatment of human corneal diseases. To resolve this problem, we expressed mutant cyclin-dependent kinase (Cdk) 4 and CyclinD1 to inactivate the pRB pathway and generate corneal endothelial cell lines without transducing viral oncogenes.

Results

HCEC with Descemet's membranes were proliferated slowly in a culture dish coated in type IV collagen. After two passages, the cells were transferred into 24-well dishes and transfected with a retroviral vector carrying E6/E7 or mutant Cdk4 and CyclinD1. Three cell lines were successfully generated, as shown in Fig. 1A, with obvious differences in growth (Fig. 1B). Protein expression from the transduced gene was confirmed by western blotting (Fig. 1C). As previously reported [21], THCEC (E6/E7) was immortalized, and THCEC (Cyclin) demonstrated the same proliferative capacity as THCEC (E6/E7), while primary cells grew more slowly even when cultured in 10% fetal bovine serum. These results indicate that induction of mutant Cdk4 and CyclinD1 is sufficient to generate a HCEC line that proliferates at a faster rate than the primary cell line.

Proliferation capacity was also confirmed by immunohistochemistry of Ki-67 (Fig. 2A). Expression of downstream genes of CyclinD1 which are associated with cell proliferation was analyzed by real-time polymerase chain reaction (PCR) (Fig. 2B). Positive staining of Ki-67, which is detected in the nucleus, was confirmed in both THCEC (Cyclin) and THCEC (E6/E7). Real-time PCR also revealed that CDC2 and PCNA, target genes of E2F (an upstream transcriptional factor), that are activated by CyclinD1, were up-regulated in THCEC (E6/E7) and especially in THCEC (Cyclin).

Expression of genes involved in active transmembrane transporter activity, including Na^+/K^+-ATPase, or cell adhesion, including ZO-1 and N-cadherin, were assessed by semi-quantitative reverse transcriptase (RT)-PCR (Fig. 3A). Expression of intercellular adhesion molecules was confirmed by immunohistochemistry (Fig. 3B–J). Semi-quantitative RT-PCR showed that there was no significant difference between the three cell lines regarding the expression of genes associated with several molecules of cell adhesion or of ion transporter channels, which are characteristically expressed by HCEC [21,24]. This was also confirmed by real-time PCR (data not shown).

ZO-1 and N-cadherin, key HCEC adhesion molecules [24], demonstrated positive staining at the intercellular junction in HCEH (Fig. 3F, I) and THCEC (Cyclin) (Fig. 3E, H), while neither ZO-1 nor N-cadherin was detected in THCEC (E6/E7) despite sufficient cellular density (Fig. 3G, J). Although positive staining of ZO-1 and N-cadherin was observed at the intercellular junction in THCEC (Cyclin), ZO-1 staining also occurred around the nucleus (Fig. 3E), indicating the immature distribution of the ZO-1 protein. In THCEC (Cyclin) and HCEC, hexagonal morphology was identified both by phase-contrast micrography (Fig. 3B, C) and immunocytochemistry, while the structure of hexagonal cell shape was not maintained in THCEC (E6/E7) (Fig. 3D). These data indicate that THCEC (Cyclin) and HCEC, but not THCEC (E6/E7), maintain contact inhibition which is crucial for preserving the monolayer.

Scanning electron microscopy was performed to reveal detailed information on the cellular junction (Fig. 4). THCEC (Cyclin) and HCEC showed a clear cellular junction including a tight junction, whereas THCEC (E6/E7) grew as a multilayer without forming a cellular junction, which confirms the immunohistochemistry result.

Representative traces of circuit current driven by the Na^+/K^+-ATPase were of similar shapes in both HCEC and THCEC (Cyclin) (Fig. 5A). These circuit currents maintain corneal translucency and their levels in both cell lines were clearly reduced by the presence of the Na^+/K^+-ATPase inhibitor ouabain, which confirms that the origin of the current is Na^+/K^+-ATPase. Meanwhile, the pump function in THCEC (Cyclin), detected in both earlier and later passages of cells, was more variable than that in HCEC (Fig. 5B), possibly indicating incomplete Na^+/K^+-ATPase activity or the presence of an intercellular barrier that regulates ion permeability. No regular circuit current was detected in THCEC (E6/E7) (Fig. 5A, B), which probably reflects the absence of intercellular adhesion preventing free ion transport across the membrane. This experiment clearly showed that the THCEC (Cyclin) monolayer has similar Na^+/K^+-ATPase activity to that of HCEC.

A tumorigenesis assay of nude mice detected no solid tumor in either THCEC (Cyclin) or THCEC (E6/E7), while HeLa cells formed a solid tumor in all mice (Table 1). Since THCEC (Cyclin) has a similar morphology and pump function to HCEC, THCEC (Cyclin) could be suitable for HCEC studies.

Discussion

THCEC (E6/E7) was shown to achieve immortalization with a highly activated proliferative capacity, as previously described [21]. However, the cell lines did not show normal intercellular contact or normal pump function, probably because contact inhibition in the cell line was not achieved. Meanwhile, THCEC (Cyclin) was demonstrated to have normal physiologic function with a greater proliferative capacity than primary cells, but slightly lower than that of THCEC (E6/E7).

In expanding the cellular life span, E7 has been shown to play a role in the inactivation of pRB, while E6 activates telomerase [25] and accelerates p53 degradation, which induces the Cdk inhibitor p21 [26]. However, little is known about the effector sites of the viral oncogene that may be related to genetic instability of immortalized cells. In the present study, expression of genes specific to HCEC was not drastically different between the three cell lines. However, key proteins including ZO-1 and N-cadherin that are important in forming intercellular contacts were detected, probably because of the unknown influence of viral oncogenes on post-translational modification, posttranslational import or protein stability/degradation.

We recently established genetically stable, non-transformed immortalized ovarian surface epithelium (OSE) cell lines without viral oncogenes by expressing mutant Cdk 4, CyclinD1 and hTERT, based on the hypothesis that inactivation of the pRb pathway and activation of telomerase are sufficient for OSE immortalization [27]. Meanwhile, Rane et al. demonstrated that mutant Cdk 4 (Cdk4R24C) is sufficient to induce carcinogenesis in several other tissues including those of the pancreas, pituitary and brain [28], and Joyce and colleagues showed that HCEC are arrested in the G1 phase and regulated by CKIs, p16INK4a and p21WAF1/Cip1 [29]. Considering the importance of maintaining

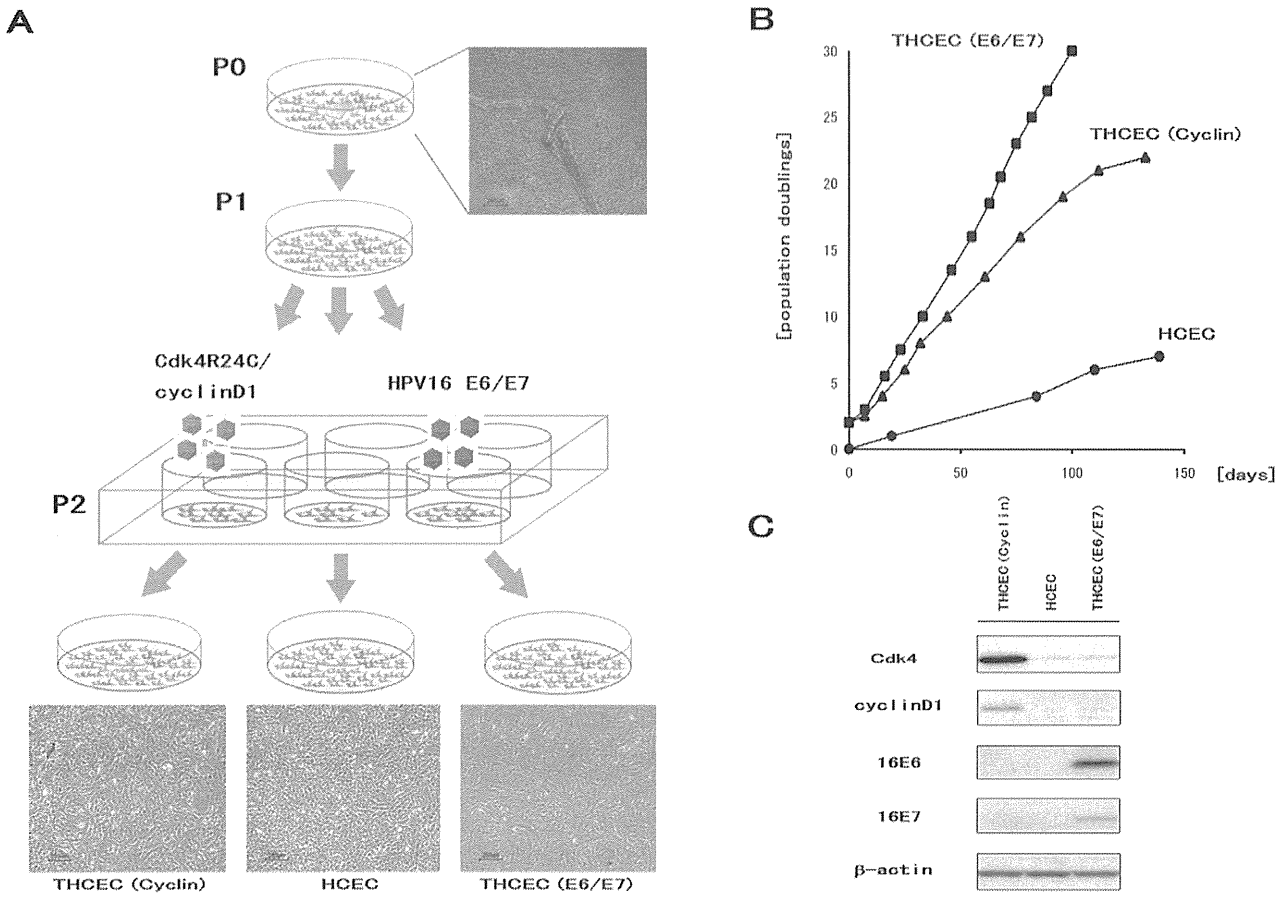

Figure 1. Establishment of THCEC (E6/E7), THCEC (Cyclin) and HCEC. (A) HCEC with Descemet's membrane were placed on Type IV collagen-coated 35 mm cell culture dishes with growth medium (P0). After one passage (P1), retroviral infection was conducted in 6-well cell culture dishes at P2. THCEC (E6/E7) and THCEC (Cyclin) were infected by retroviral vectors carrying HPV16 E6/E7 and both CyclinD1 and Cdk4R24C, respectively. (B) Growth curves of THCEC (E6/E7), THCEC (Cyclin) and HCEC cell lines. THCEC (E6/E7) was immortalized as reported previously, and THCEC (Cyclin) obtained the same proliferative activity as that of THCEC (E6/E7). Transfection was performed on day 0 for THCEC (E6/E7) and THCEC (Cyclin), with population doublings of 2. For HCEC, primary culture commenced on day 0. (C) Western blotting confirmed the expression of the following transgenes: E6 and E7 in THCEC (E6/E7), and CyclinD1 and Cdk4R24C in THCEC (Cyclin).
doi:10.1371/journal.pone.0029677.g001

morphology and physiologic function in HCEC, we only transduced mutant Cdk 4 and CyclinD1, not hTERT, in the present study. We believe that our careful method enabled THCEC (Cyclin) to form a fragile and regularly arranged monolayer complete with physiologic function.

Although THCEC (Cyclin) has similar characteristics to primary HCEC, immunohistochemistry and the Ussing chamber assay also highlighted the differences between the cells. ZO-1 protein was expressed around the nucleus of THCEC (Cyclin) but not in primary cells. Since semi-quantitative PCR detected almost the same level of mRNA expression between the cell lines, staining around the nucleus in THCEC (Cyclin) probably reflects an error in posttranslational import of ZO-1 protein. The Ussing chamber assay detected a similar pump function between THCEC (Cyclin) and primary cells, but the current in THCEC (Cyclin) was more variable than that of the primary cells, which might have been caused by reduced Na^+/K^+-ATPase activity, immature intercellular adhesion allowing irregular intercellular ion transport or differences in cellular density.

Cells established by a retrovirus carry a potential risk of promoting carcinogenesis [30], and direct transplantation to humans of cell sheets composed of such cells may lead to complex problems. Recently, to resolve this problem, several studies have reported the establishment of untransfected corneal endothelial cell lines [31,32,33], which are the most ideal cell lines for the treatment of human corneal disease. Meanwhile, alternative bioengineering approaches, including lipofection of p27kip1 siRNA [34], proteomics technology analyzing the difference between younger and older HCEC [35] and drug usage of promyelocytic leukemia zinc finger protein, a cell cycle transcriptional repressor and negative regulator [36], have also been introduced. The present findings support the idea that targeting the interaction between p16INK4a and Cdk4 using such methods is a promising strategy to generate HCEC with sufficient proliferative capacity and physiologic function.

Materials and Methods

Isolation and cell culture of human corneal cells

Ethics Statement. A cornea was excised from the surgically enucleated eye of a 2-year-old infant undergoing therapy for retinoblastoma, with the approval (approval number, #156) of the

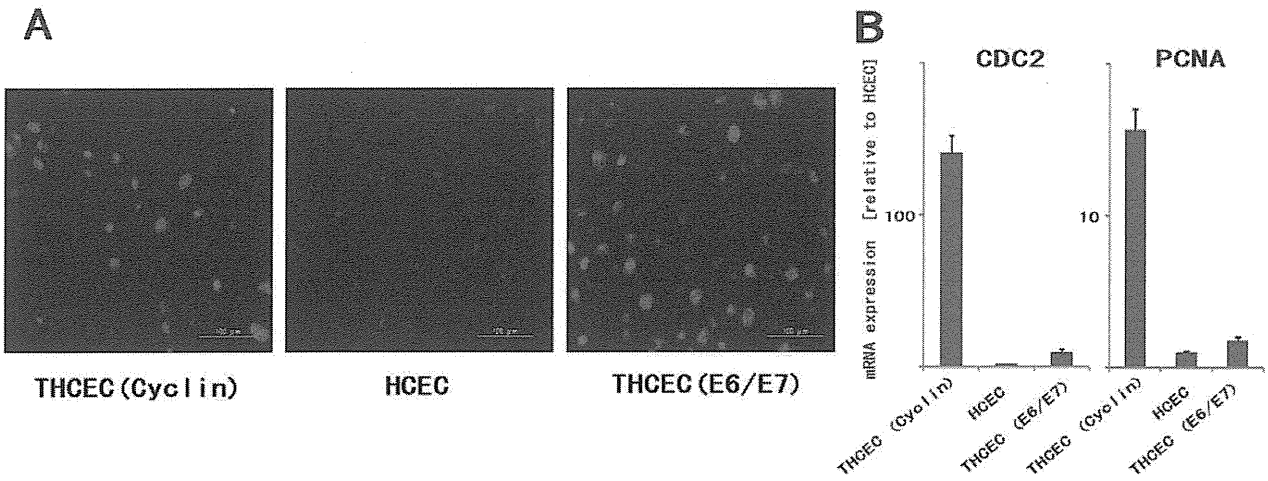

Figure 2. Evaluation of proliferative capacity. (A) Immunohistochemistry of Ki-67 in three cell lines. Positive staining of Ki-67, located in the nucleus, was obviously identified in THCEC (Cyclin) and THCEC (E6/E7), but rarely detected in HCEC. (B) Real-time PCR of downstream genes of cyclinD1 associated with proliferation. Gene expression levels of both CDC2 and PCAN were clearly higher than that of HCEC. The gene expression was much more activated in THCEC (Cyclin) in which the expression of E2F, an upstream transcriptional factor of two genes, was constitutively activated by transduced mutant Cdk4 and CyclinD1.
doi:10.1371/journal.pone.0029677.g002

Ethics Committee of the National Institute for Child and Health Development, Tokyo, Japan. Signed informed consent was obtained from the donor's parents, and the surgical specimens were irreversibly de-identified. All experiments handling human cells and tissues were performed in line with the tenets of the Declaration of Helsinki.

The corneal piece, which was grossly normal with no pathological lesions, was cut 1.5 mm from the corneal limbus,

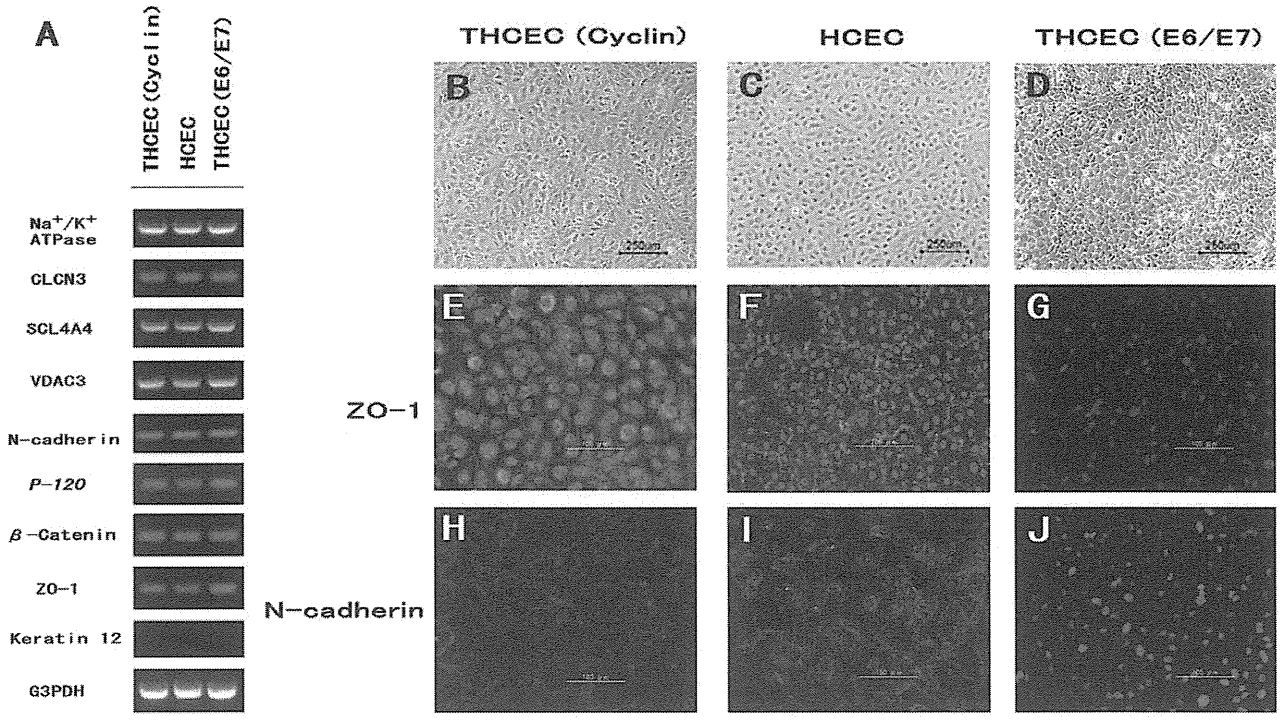

Figure 3. HCEC-associated genes and cytolocalization of junctional components expressed by cell lines. (A) Semi-quantitative reverse transcriptase polymerase chain reaction for HCEC-associated genes. Total RNA was prepared from cultured cells seven days after reaching confluency. No significant difference in mRNA expression was observed between the three cell lines. Compared with phase-contrast micrographs of (B) THCEC (Cyclin), (C) HCEC and (D) THCEC (E6/E7), cytolocalization was examined by immunofluorescence staining of ZO-1 (E, F,G) and N-cadherin (H, I, J). THCEC (E6/E7) did not stain positive for intercellular junctional molecules, while ZO-1 and N-cadherin stained positive at the junction in THCEC (Cyclin) and HCEC.
doi:10.1371/journal.pone.0029677.g003

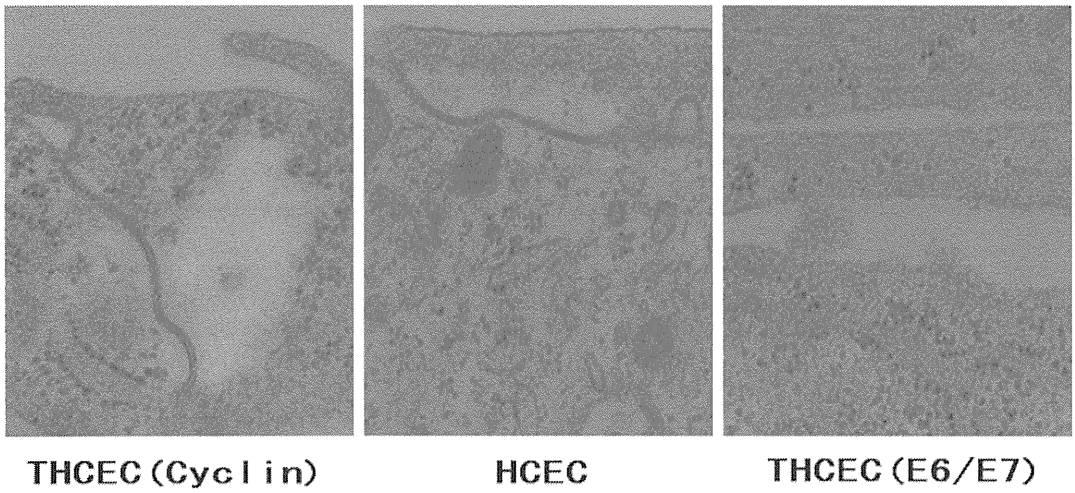

Figure 4. Transmission electron microscopy of cell line intercellular junctions. The junctional complex was detected at the intercellular junction in THCEC (Cyclin) and HCEC. No component of the intercellular junction was found in THCEC (E6/E7), in which cells grew in multilayers without being inhibited by cellular contact (scale bar = 200 nm).
doi:10.1371/journal.pone.0029677.g004

avoiding contamination of the trabecular meshwork tissue. HCEC with Descemet's membrane were stripped from the posterior surface of the corneal tissue with sterile surgical forceps under a dissecting microscope. They were cut into two pieces and cultured in a cell culture dish covered with Type IV collagen in a growth medium (GM); Dulbecco's modified Eagle's medium (DMEM)/Nutrient mixture F12 (1:1) with high glucose supplemented with 10% fetal bovine serum, insulin-transferrin-selenium and MEM-NEAA (Gibco, Auckland, NZ). Cells were subcultured after reaching confluency by treating with trypsin/EDTA and seeded at a density of 5×10^5 cells/well in 6-well dishes.

Viral vector construction and viral transduction

Lentiviral vector plasmids, CSII-CMV-cyclin D1 and -CDK4R24C were constructed by recombination using the Gateway system (Invitrogen, Carlsbad, CA) as described previously [37]. Briefly, cDNAs of human cyclinD1 and a mutant form of Cdk4 (Cdk4R24C: an inhibitor resistant form of Cdk4, generously provided by Dr Hara) were recombined with a lentiviral vector, CSII-CMV-RfA (a gift from Dr Miyoshi), by LR reaction to create a Gateway expression plasmid (Invitrogen) according to the manufacturer's instructions.

Previous work has described the production of recombinant lentiviruses with the vesicular stomatitis virus G glycoprotein [37], the recombinant retrovirus vector plasmid, pCLXSN-16E6E7 encoding HPV16 E6/E7 (16E6E7) [38] and recombinant retroviruses [39]. Following the addition of recombinant viral fluid to cells seeded in 24-well dishes in the presence of 4 μg/ml polybrene, the cells were infected by the viruses. Stably transduced cells with an expanded life span were designated transduced

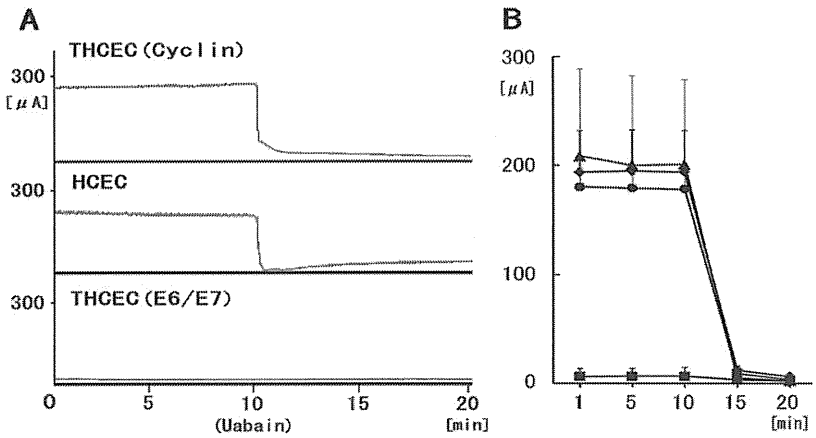

Figure 5. The pump function of cell lines. Short-circuit currents representing Na^+/K^+-ATPase activity from corneal cell monolayers on the insert well area of 4.67 cm^2 were calculated before and after addition of the Na^+/K^+-ATPase inhibitor ouabain. (A) Representative tracings of short-circuit current (μA/well) obtained with cell monolayers of THCEC (Cyclin) (upper panel), HCEC (middle panel) and THCEC (E6/E7) (lower panel). THCEC (Cyclin) possessed equal transport activity to HCEC, whereas no pump function was detected in THCEC (E6/E7). (B) Time-course changes in the average short circuit current of cultured monolayers of cell lines at 1, 5, 10 and 20 min. Data shown are for (▲) THCEC (Cyclin) at PD8, (♦) THCEC (Cyclin) at PD 21, (•) HCEC and (■) THCEC (E6/E7); all data are expressed as mean±SD of four replicate experiments of each cell line.
doi:10.1371/journal.pone.0029677.g005

Table 1. Tumorigenesis assay of cell lines in BALB/C nude mice.

Inoculated cells	Total dose (cell/mouse)	Number of mice (% mortality)	Number of mice with tumor
THCEC (Cyclin)	1.7×10^6	3(0)	0
THCEC (E6/E7)	1.7×10^6	3(0)	0
HeLa cells	2.0×10^6	3(0)	3

doi:10.1371/journal.pone.0029677.t001

human corneal endothelial cell by E6/E7 (THCEC (E6/E7)) and transduced human corneal endothelial cell by Cdk4R24C/cyclinD1 (THCEH (Cyclin)).

Culture of transfected cell lines and growth curve

When the cultures reached subconfluence, the cells were harvested with 0.25% trypsin and 1 mM EDTA, collected into tubes, and centrifuged. The cells were counted using a cell viability analyzer (Vi-CELL Cell Viability Analyzer, Beckman Coulter, Brea, CA), and population doubling (PD) was calculated. The pellets were suspended in growth medium, and the cells were passaged at a density of 5×10^5 cells/well in a 100-mm dish. The original cells were regarded as PD 2 (day 0).

Western blot analysis

Western blotting was conducted as described previously [40]. Antibodies against Cdk4 (ser473; Cell Signaling Technology, Danvers, MA), CyclinD1 (clone G124-326; BD Biosciences, Franklin Lakes, NJ), β-actin (sc-1616; Santa Cruz Biotechnology, Santa Cruz, CA) were used as probes, and horseradish peroxidase-conjugated anti-mouse, anti-rabbit (Jackson Immunoresearch Laboratories, West Grove, PA) or anti-goat (sc-2033; Santa Cruz Biotechnology, Santa Cruz, CA) immunoglobulins were employed as secondary antibodies.

Immunocytochemistry

Cell lines were grown on Type IV collagen-coated glass dishes 14 days after reaching confluency and were fixed with 4% formaldehyde (pH 7.0) for 15 min at room temperature. Cell lines were then rehydrated in phosphate buffered saline (PBS), incubated with 0.2% Triton X-100 for 15 min and rinsed three times with PBS for 5 min each. After incubation with 2% BSA to block nonspecific staining for 30 min, cell lines were incubated with anti-ZO-1 (1:50; sc-8146; Santa Cruz Biotechnology, Santa Cruz, CA), anti-N-cadherin (1:50; sc-7939; Santa Cruz Biotechnology) and anti-Ki67 (1:100; ab15580; Abcam, Cambridge, UK) for 16 h at 4°C. After three washes with PBS, cell lines were incubated with the secondary antibody for 60 min, followed by counterstaining with 4′,6-diamidino-2-phenylindole (1:200; sc-3598; Santa Cruz Biotechnology) for 10 min.

Semi-quantitative RT-PCR

Total RNA was extracted from 1×10^6 cultured HCEC using the RNeasy Plus mini-kitH (Qiagen, Germantown/Gaithersburg, MA) according to the manufacturer's instructions and quantified by absorption at 260 nm. Total RNA was then reverse-transcribed into cDNA using Superscript III Reverse Transcriptase (Invitrogen, Carlsbad, CA) with oligo random hexamers. cDNAs of each component were amplified by PCR using specific primers and DNA polymerase. The reaction was first incubated at 95°C for 10 min, followed by 39 cycles at 98°C for 30 s, 58°C for 30 s and 74°C for 30 s. PCR primers are listed in Table 2.

Quantitative real-time RT-PCR

Total RNA extraction and reverse transcription into cDNA was carried out as above. Each quantitative real-time RT-PCR for target genes, including Cell Division Cycle 2 (*CDC2*) and proliferating cell nuclear antigen (*PCNA*), was performed using the Chromo4 real time detection system (Bio-Rad, Hercules, CA). For a 20 ml PCR, the cDNA template was mixed with the primers to final concentrations of 200 nM and 10 μl of SsoFast EvaGreen Supermix (BIO-RAD), respectively. The reaction was first incubated at 95°C for 10 min, followed by 45 cycles at 95°C for 10 s, 57°C for 15 s, and 72°C for 20 s.

Transmission Electron Microscopy

Cell lines cultured on Type IV collagen-coated dishes were fixed in HEPES buffered 2% glutaraldehyde and subsequently post-fixed in 2% osmium tetroxide for 3 h on ice. Specimens were then dehydrated in graded ethanol and embedded in the epoxy resin. Ultrathin sections were obtained by ultramicrotomy and stained with uranyl acetate for 10 min and modified Sato's lead solution for 5 min then submitted to TEM observation (JEM-2000EX, JEOL).

Measurement of pump function

The pump function of confluent monolayers of HCEC was measured using an Ussing chamber as described previously [41]. Cells cultured on Snapwell inserts coated with Type IV collagen were placed in the Ussing chamber EM-CSYS-2 (Physiologic Instruments, San Diego, CA) with the endothelial cell surface side in contact with one chamber and the Snapwell membrane side in contact with another chamber. The chambers were carefully filled with Krebs-Ringer bicarbonate (120.7 mM NaCl, 24 mM $NaHCO_3$, 4.6 mM KCl, 0.5 mM $MgCl_2$, 0.7 mM Na_2HPO_4, 1.5 mM NaH_2PO_4 and 10 mM glucose bubbled with a mixture of 5% CO_2, 7% O_2 and 88% N_2 to pH 7.4). The chambers were maintained at 37°C using an attached heater.

The short-circuit current was sensed by narrow polyethylene tubes positioned close to either side of the Snapwell, filled with 3 M KCl and 4% agar gel and connected to silver electrodes. These electrodes were connected to the computer through the Ussing system VCC-MC2 (Physiologic Instruments) and an iWorx 118 Research Grade Recorder (iWorx Systems, Dover, NH), and the short-circuit current was recorded by Labscribe2 Software for Research (iWorx). After the short-circuit current had reached a steady state, ouabain (final concentration, 1 mM) was added to the chamber, and the short-circuit current was re-measured. The pump function attributable to Na^+/K^+-ATPase activity was calculated as the difference in short-circuit current measured before and after the addition of ouabain.

Tumorigenesis assay

Cells were harvested by Trypsin/EDTA treatment, collected into tubes, and centrifuged, and the pellets were suspended in

Table 2. Oligonucleotide sequences for RT-PCR.

Name	Sequence	Size (bp)	Accession Number
Collagen type IV	F: 5′-GGC ACC TGC CAC TAC TAC GC-3′	472	NM_001845
	R: 5′-TCA CCA GGA GGT AGC CGA T-3′		
Keratin 12	F: 5′-GAT GCT AAT GCT GAG CTC GA-3′	393	NM_000223
	R: 5′-ACC TGC CCT ACA GCT TTG TA-3		
VDAC3	F: 5′-TGA CTC TTG ATA CCA TAT TTG TAC CG-3′	482	NM_001135694
	R: 5′-TCA ATT TGA CTC CTG GTC GAA-3′		
CLCN3	F: 5′-AGA AAG GCA TAG ACG GAT CAA-3′	204	NM_001829
	R: 5′-GGT TGT ACC ACA ACG CAC TAA-3′		
SLC4A4	F: 5′-GTT CAG ATG AAT GGG GAT ACGC	697	NM_001136260
	R: 5′-CGA GCA TAA ACA CAA AGC GTA A-3′		
Na^+/K^+-ATPase	F: 5′-CCC AGG ACT CAT GGT TTT TC-3′	482	NM_000702
	R: 5′-GGA GCA AAG CTG ACC TGA AC-3′		
N-cadherin	F: 5′-CAA CTT GCC AGA AAA CTC CAG G-3′	205	NM_ 001792
	R: 5′-ATG AAA CCG GGC TAT CTG CTC-3′		
β-catenin	F: 5′-TAC CTC CCA AGT CCT GTA TGA G-3′	180	NM_001904
	R: 5′-TGA GCA GCA TCA AAC TGT GTA G-3′		
P-120	F: 5′-CCC CAG GAT CAC AGT CAC CT-3′	144	NM_001085467
	R: 5′-CCG AGT GGT CCC ATC ATC TG-3′		
ZO-1	F: 5′-AGT CCC TTA CCT TTC GCC TGA-3′	180	NM_003257
	R: 5′-TCT CTT AGC ATT ATG TGA GCT GC-3′		
GAPDH	F: 5′-GCT CAG ACA CCA TGG GGA AGG T-3′	474	NM_002046
	R: 5′-GTG GTG CAG GAG GCA TTG CTG A-3′		
PCNA	F: 5′- GCGTGAACCTCACCAGTATGT-3′	76	NM_002592
	R: 5′- TCTTCGGCCCTTAGTGTAATGAT-3′		
CDC2	F: 5′- GGATGTGCTTATGCAGGATTCC-3′	100	NM_001786
	R: 5′- CATGTACTGACCAGGAGGGATAG-3′		

VDAC3: voltage-dependent anion channel 3, CLCN3: chloride channel protein 3, SLC4A4: sodium bicarbonate cotransporter membrane.
doi:10.1371/journal.pone.0029677.t002

DMEM. The same volume of Basement Membrane Matrix (BD Biosciences) was added to the cell suspension. Cells (1.7×10^6) of THCEC (Cyclin) and THCEC (E6/E7) were inoculated subcutaneously into dorsal flanks of each of three Balb/c nu/nu mice (CREA, Japan) for 60 days. A total of 2.0×10^6 HeLa cells per mouse were used as positive controls. The skin of dorsal flanks of inoculated mice was surgically opened and the tumorigenic status was examined.

Author Contributions

Conceived and designed the experiments: Tadashi Yokoi YS Tae Yokoi TK AU HN NA. Performed the experiments: Tadashi Yokoi YS Tae Yokoi HM SH MY TK HN NA. Analyzed the data: Tadashi Yokoi YS Tae Yokoi HM SH MY AU HN NA. Contributed reagents/materials/analysis tools: Tadashi Yokoi SH MY TK HN NA. Wrote the paper: Tadashi Yokoi YS TK AU HN NA.

References

1. Hatou S, Yamada M, Mochizuki H, Shiraishi A, Joko T, et al. (2009) The effects of dexamethasone on the Na,K-ATPase activity and pump function of corneal endothelial cells. Curr Eye Res 34: 347–354.
2. Barfort P, Maurice D (1974) Electrical potential and fluid transport across the corneal endothelium. Exp Eye Res 19: 11–19.
3. Bourne WM, Nelson LR, Hodge DO (1997) Central corneal endothelial cell changes over a ten-year period. Invest Ophthalmol Vis Sci 38: 779–782.
4. Hashemian MN, Moghimi S, Fard MA, Fallah MR, Mansouri MR (2006) Corneal endothelial cell density and morphology in normal Iranian eyes. BMC Ophthalmol 6: 9.
5. Padilla MD, Sibayan SA, Gonzales CS (2004) Corneal endothelial cell density and morphology in normal Filipino eyes. Cornea 23: 129–135.
6. Adamis AP, Filatov V, Tripathi BJ, Tripathi RC (1993) Fuchs' endothelial dystrophy of the cornea. Surv Ophthalmol 38: 149–168.
7. Schultz RO, Matsuda M, Yee RW, Edelhauser HF, Schultz KJ (1984) Corneal endothelial changes in type I and type II diabetes mellitus. Am J Ophthalmol 98: 401–410.
8. Slingsby JG, Forstot SL (1981) Effect of blunt trauma on the corneal endothelium. Arch Ophthalmol 99: 1041–1043.
9. Bourne WM, Nelson LR, Hodge DO (1994) Continued endothelial cell loss ten years after lens implantation. Ophthalmology 101: 1014–1022;discussion 1022–1013.
10. Gagnon MM, Boisjoly HM, Brunette I, Charest M, Amyot M (1997) Corneal endothelial cell density in glaucoma. Cornea 16: 314–318.
11. Laing RA, Sanstrom MM, Berrospi AR, Leibowitz HM (1976) Changes in the corneal endothelium as a function of age. Exp Eye Res 22: 587–594.
12. Landshman N, Ben-Hanan I, Assia E, Ben-Chaim O, Belkin M (1988) Relationship between morphology and functional ability of regenerated corneal endothelium. Invest Ophthalmol Vis Sci 29: 1100–1109.
13. Coster DJ, Williams KA (2005) The impact of corneal allograft rejection on the long-term outcome of corneal transplantation. Am J Ophthalmol 140: 1112–1122.
14. Terry MA, Ousley PJ (2001) Deep lamellar endothelial keratoplasty in the first United States patients: early clinical results. Cornea 20: 239–243.
15. Price FW Jr., Price MO (2005) Descemet's stripping with endothelial keratoplasty in 50 eyes: a refractive neutral corneal transplant. J Refract Surg 21: 339–345.
16. Melles GR, Ong TS, Ververs B, van der Wees J (2006) Descemet membrane endothelial keratoplasty (DMEK). Cornea 25: 987–990.

17. Zhu C, Joyce NC (2004) Proliferative response of corneal endothelial cells from young and older donors. Invest Ophthalmol Vis Sci 45: 1743–1751.
18. Li W, Sabater AL, Chen YT, Hayashida Y, Chen SY, et al. (2007) A novel method of isolation, preservation, and expansion of human corneal endothelial cells. Invest Ophthalmol Vis Sci 48: 614–620.
19. Ishino Y, Zhu C, Harris DL, Joyce NC (2008) Protein tyrosine phosphatase-1B (PTP1B) helps regulate EGF-induced stimulation of S-phase entry in human corneal endothelial cells. Mol Vis 14: 61–70.
20. Senoo T, Joyce NC (2000) Cell cycle kinetics in corneal endothelium from old and young donors. Invest Ophthalmol Vis Sci 41: 660–667.
21. Kim HJ, Ryu YH, Ahn JI, Park JK, Kim JC (2006) Characterization of immortalized human corneal endothelial cell line using HPV 16 E6/E7 on lyophilized human amniotic membrane. Korean J Ophthalmol 20: 47–54.
22. Nitta M, Katabuchi H, Ohtake H, Tashiro H, Yamaizumi M, et al. (2001) Characterization and tumorigenicity of human ovarian surface epithelial cells immortalized by SV40 large T antigen. Gynecol Oncol 81: 10–17.
23. Tsao SW, Mok SC, Fey EG, Fletcher JA, Wan TS, et al. (1995) Characterization of human ovarian surface epithelial cells immortalized by human papilloma viral oncogenes (HPV-E6E7 ORFs). Exp Cell Res 218: 499–507.
24. Zhu YT, Hayashida Y, Kheirkhah A, He H, Chen SY, et al. (2008) Characterization and comparison of intercellular adherent junctions expressed by human corneal endothelial cells in vivo and in vitro. Invest Ophthalmol Vis Sci 49: 3879–3886.
25. Kiyono T, Foster SA, Koop JI, McDougall JK, Galloway DA, et al. (1998) Both Rb/p16INK4a inactivation and telomerase activity are required to immortalize human epithelial cells. Nature 396: 84–88.
26. Sekiguchi T, Hunter T (1998) Induction of growth arrest and cell death by overexpression of the cyclin-Cdk inhibitor p21 in hamster BHK21 cells. Oncogene 16: 369–380.
27. Sasaki R, Narisawa-Saito M, Yugawa T, Fujita M, Tashiro H, et al. (2009) Oncogenic transformation of human ovarian surface epithelial cells with defined cellular oncogenes. Carcinogenesis 30: 423–431.
28. Rane SG, Cosenza SC, Mettus RV, Reddy EP (2002) Germ line transmission of the Cdk4(R24C) mutation facilitates tumorigenesis and escape from cellular senescence. Mol Cell Biol 22: 644–656.
29. Enomoto K, Mimura T, Harris DL, Joyce NC (2006) Age differences in cyclin-dependent kinase inhibitor expression and rb hyperphosphorylation in human corneal endothelial cells. Invest Ophthalmol Vis Sci 47: 4330–4340.
30. Robinson HL (1982) Retroviruses and cancer. Rev Infect Dis 4: 1015–1025.
31. Fan T, Zhao J, Ma X, Xu X, Zhao W, et al. (2011) Establishment of a continuous untransfected human corneal endothelial cell line and its biocompatibility to denuded amniotic membrane. Mol Vis 17: 469–480.
32. Fan T, Wang D, Zhao J, Wang J, Fu Y, et al. (2009) Establishment and characterization of a novel untransfected corneal endothelial cell line from New Zealand white rabbits. Mol Vis 15: 1070–1078.
33. Valtink M, Gruschwitz R, Funk RH, Engelmann K (2008) Two clonal cell lines of immortalized human corneal endothelial cells show either differentiated or precursor cell characteristics. Cells Tissues Organs 187: 286–294.
34. Kikuchi M, Zhu C, Senoo T, Obara Y, Joyce NC (2006) p27kip1 siRNA induces proliferation in corneal endothelial cells from young but not older donors. Invest Ophthalmol Vis Sci 47: 4803–4809.
35. Zhu C, Rawe I, Joyce NC (2008) Differential protein expression in human corneal endothelial cells cultured from young and older donors. Mol Vis 14: 1805–1814.
36. Shiraishi A, Joko T, Higashiyama S, Ohashi Y (2007) Role of promyelocytic leukemia zinc finger protein in proliferation of cultured human corneal endothelial cells. Cornea 26: S55–58.
37. Miyoshi H, Blomer U, Takahashi M, Gage FH, Verma IM (1998) Development of a self-inactivating lentivirus vector. J Virol 72: 8150–8157.
38. Narisawa-Saito M, Yoshimatsu Y, Ohno S, Yugawa T, Egawa N, et al. (2008) An in vitro multistep carcinogenesis model for human cervical cancer. Cancer Res 68: 5699–5705.
39. Naviaux RK, Costanzi E, Haas M, Verma IM (1996) The pCL vector system: rapid production of helper-free, high-titer, recombinant retroviruses. J Virol 70: 5701–5705.
40. Haga K, Ohno S, Yugawa T, Narisawa-Saito M, Fujita M, et al. (2007) Efficient immortalization of primary human cells by p16INK4a-specific short hairpin RNA or Bmi-1, combined with introduction of hTERT. Cancer Sci 98: 147–154.
41. Mimura T, Yamagami S, Yokoo S, Usui T, Tanaka K, et al. (2004) Cultured human corneal endothelial cell transplantation with a collagen sheet in a rabbit model. Invest Ophthalmol Vis Sci 45: 2992–2997.

Vernal Keratoconjunctivitis With Giant Papillae on the Inferior Tarsal Conjunctiva

Yosuke Asada, MD, Nobuyuki Ebihara, MD, PhD,* Toshinari Funaki, MD, PhD,* Norihiko Yokoi, MD, PhD,† Akira Murakami, MD, PhD,* and Akira Matsuda, MD, PhD**

Purpose: In vernal keratoconjunctivitis (VKC), giant papillae are commonly observed on the superior tarsal conjunctiva. We found 3 cases of giant papillae on the inferior tarsal conjunctiva, and diagnosed them as being VKC based on their clinical and histopathological features.

Methods: Three patients with inferior tarsal giant papillae were studied. In 2 patients, the giant papillae were resected for therapeutic purposes. Immunohistochemical analysis was carried out by indirect immunofluorescent staining using anti-CD3, anti-CD20, anti-CD35 antibodies.

Results: In all 3 patients, giant papilla formation was observed on the inferior lid margin. Clusters of $CD20^+$ B lymphocytes with $CD35^+$ follicular dendritic cells, and $CD3^+$ marginal zone T lymphocytes, common features of lymphoid neogenesis, were observed. In 2 patients, typical giant papillary formation was also observed on the superior tarsal conjunctiva. In all the patients, topical dexamethasone and tacrolimus treatments were found to be effective.

Conclusions: The giant papillae of VKC can occur not only on the superior tarsal conjunctiva but also on the inferior tarsal conjunctiva. The possibility of the presence of giant papillae on the inferior tarsal conjunctiva should be considered in the clinical examination of patients with VKC.

Key Words: vernal keratoconjunctivitis

(*Cornea* 2014;33:32–34)

In vernal keratoconjunctivitis (VKC), giant papillae are commonly observed on the superior tarsal conjunctiva. Bonini et al[1] reported that 163 (83.6%) of 195 patients with VKC had papillary formation on the upper tarsal conjunctiva, and 16.4% of the patients had giant papillary formation. A limbal form of VKC is also known. Trantas dots are a typical sign of the limbal form of VKC with epithelial cells and eosinophil accumulation.[2] Involvement of the lower tarsal conjunctiva is common in atopic keratoconjunctivitis; however, giant papillary formations on the lower tarsal conjunctiva have not been reported. We examined 3 cases of VKC with giant papillary formation on the inferior tarsal conjunctiva. Histological analysis showed eosinophil and mast cell infiltration in the tissue, and tertiary lymphoid organ (TLO) formation as reported for giant papillae on the upper tarsal conjunctivae.[3]

Received for publication April 8, 2013; revision received August 15, 2013; accepted September 16, 2013. Published online ahead of print November 14, 2013.

From the *Department of Ophthalmology, Juntendo University Graduate School of Medicine, Tokyo, Japan; and †Department of Ophthalmology, Kyoto Prefectural University of Medicine, Kyoto, Japan.

Supported in part by Grants-in-aid from the Japan Society for the Promotion of Science (No. 24592652 to A.Ma., 24659768 to A.Mu.), the Takeda Science Foundation (A.Ma.), and the Institute for Environmental and Gender-specific Medicine, Juntendo University (A.Ma.).

The authors have no funding or conflicts of interest to disclose.

Supplemental digital content is available for this article. Direct URL citations appear in the printed text and are provided in the HTML and PDF versions of this article on the journal's Web site (www.corneajrnl.com).

Reprints: Akira Matsuda, Laboratory of Ocular Atopic Diseases, Department of Ophthalmology, Juntendo University School of Medicine, 2-1-1 Hongo, Bunkyo-Ku, Tokyo 113-8431, Japan (e-mail: akimatsu@juntendo.ac.jp).

MATERIALS AND METHODS

Giant Papilla Samples

Giant papillae were resected from 2 patients with VKC for therapeutic purposes. During the resection surgery, the tissue was obtained after the patients gave written informed consent as previously described.[4] All the procedures were approved by the ethics committees of the Juntendo University School of Medicine and Kyoto Prefectural University of Medicine, and the study was conducted in accordance with the tenets of the Declaration of Helsinki. VKC was defined as a chronic, bilateral, conjunctival inflammatory condition found in individuals as previously described.[4]

Cytological Analysis

Conjunctival smears were prepared using an ophthalmic spatula and glass slides. Hansel staining was carried out to detect eosinophils using Eosinostain (Torii Pharmaceutical Co, Ltd, Tokyo, Japan) according to the manufacturer's protocol.

Immunohistochemical Analysis

Immunohistochemical staining was carried out essentially as previously described.[3] Mouse antihuman CD3, antihuman CD35 monoclonal antibodies (Dako Japan, Kyoto, Japan), and a rabbit CD20 monoclonal antibody (Epitomics, Burlingame, CA) were used as primary antibodies. Negative control staining was carried out using isotype-matched immunoglobulin G (IgG) as substitutes for the primary antibodies.

RESULTS

Presentation of Cases

Case 1

A 16-year-old female with chronic itchiness and a foreign body sensation was referred to our clinic. On initial examination, we found giant papillae at the lid margins of the inferior tarsal conjunctivae of both eyes (Figs. 1A, B). She did not have any other atopic manifestations (asthma or atopic dermatitis). We found eosinophil infiltration of conjunctival smears obtained from her inferior tarsal conjunctivae, and identified eosinophils by Hansel staining (Fig. 1A inset, arrow). We could not find giant papillae on her superior tarsal conjunctivae, but mild scar formation was observed at the initial examination (Fig. 1C). The giant papillae in the inferior tarsal conjunctivae of both eyes were resected for therapeutic purposes. No corneal involvement was observed. Topical dexamethasone and tacrolimus eye drops were started, and her symptoms were well controlled. After several months, typical cobblestone-like giant papillae were observed on the upper tarsal conjunctivae of both eyes (Fig. 1D). Laboratory tests showed no abnormality except high total serum IgE (509 IU/mL). Histological analysis by hematoxylin–eosin staining showed large lymphatic follicle formation (see Figure, Supplemental Digital Content 1, http://links.lww.com/ICO/A164, arrow) and infiltration of eosinophils in the giant papillae (see Figure, Supplemental Digital Content 2, http://links.lww.com/ICO/A164, arrows). Immunohistochemical analysis showed major basic protein-positive eosinophil infiltration (see Figure, Supplemental Digital Content 3, http://links.lww.com/ICO/A164) and IgE- and high affinity IgE receptor beta (FcεRIβ)-double-positive mast cells were observed within and beneath the conjunctival epithelium (see Figure, Supplemental Digital Content 4, http://links.lww.com/ICO/A164).

Case 2

A 13-year-old male with chronic itchiness and foreign body sensation was referred to our clinic. We found a giant papillary formation on the inferior tarsal conjunctivae (Figs. 2A, B). He did not have any other atopic manifestations (asthma or atopic dermatitis). Laboratory tests showed no abnormality except high total serum IgE (2319 IU/mL). The giant papillae of the inferior tarsal conjunctivae of both eyes were resected for therapeutic purposes. Topical dexamethasone and tacrolimus eye drops were started, and his symptoms were well controlled. Immunohistochemical analysis revealed CD3-positive T lymphocytes around CD20-positive B cells clusters (Fig. 2C), and CD20-positive B lymphocyte (B cells) clusters with CD35-positive follicular dendritic cells (FDCs; Fig. 2D).

Case 3

An 11-year-old male with chronic swelling of the left inferior eyelid had been treated for chalazion for 2 years. He was referred to our clinic for treatment of an eyelid tumor. He also complained of having chronic itchiness. We found a giant papilla at the lid margin of his left inferior tarsal conjunctiva (see Figure, Supplemental Digital Content 5, http://links.lww.com/ICO/A165). In addition, typical cobblestone-like giant papillae were observed on his right superior tarsal conjunctiva (see Figure, Supplemental Digital Content 6, http://links.lww.com/ICO/A165). He did not have any other atopic manifestations (asthma or atopic dermatitis). Topical dexamethasone and tacrolimus eye drops were started, causing the giant papillae of both inferior and superior tarsal conjunctivae to regress after 2 weeks of treatment, and his symptoms were well controlled.

DISCUSSION

We found 3 cases of VKC with giant papillary formation on the inferior tarsal conjunctiva. All 3 patients

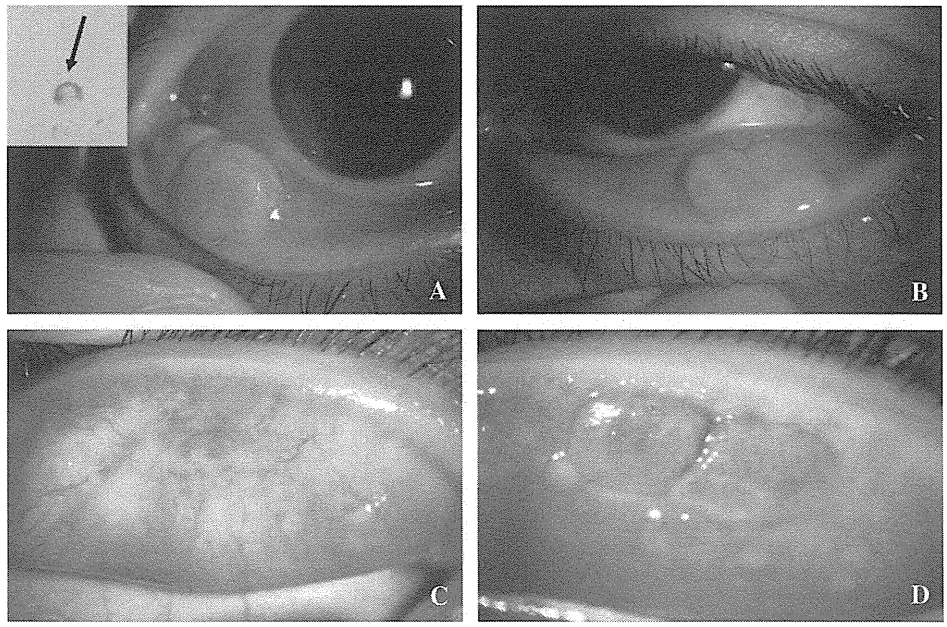

FIGURE 1. Giant papillary formation on the inferior tarsal conjunctivae in case 1. A giant papillary formation was observed in the right eye (A) and left eye (B). Note that the giant papillae were located at the lid margin. Hansel staining of a conjunctival smear shows eosinophilic granules (arrow in the inset, A). The upper tarsal conjunctiva of the right eye shows scar formation (C), and that of the left eye shows typical cobblestone-like giant papillae (D).

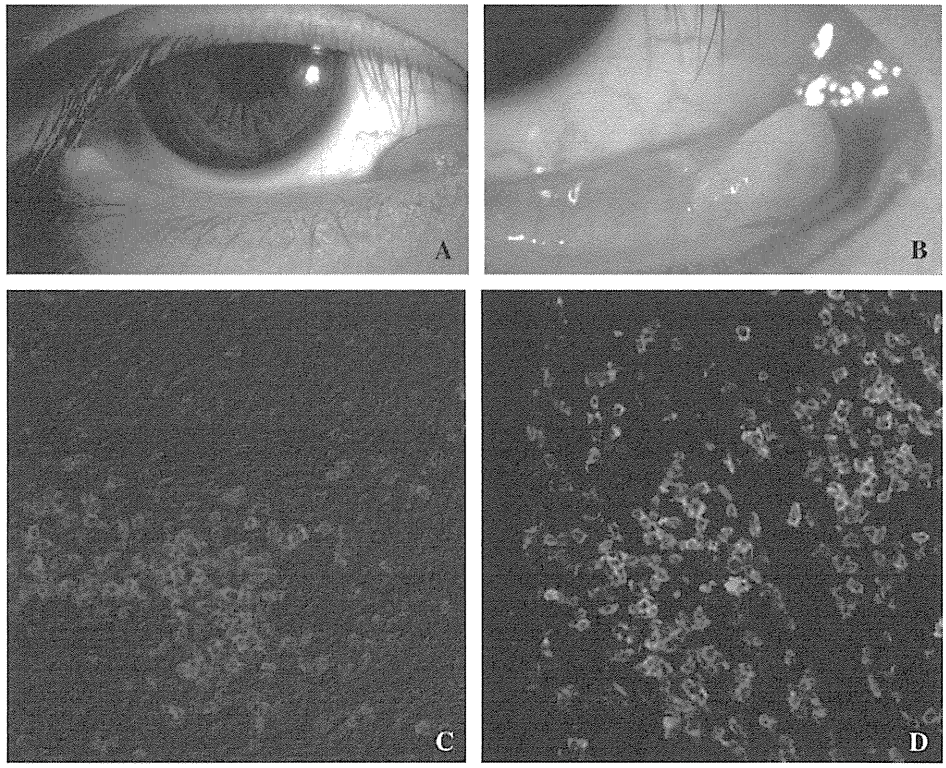

FIGURE 2. Giant papillary formation on the inferior tarsal conjunctivae in case 2, and immunohistological analysis. Giant papillary formation can be observed in the right eye (A) and left eye (B). Note the giant papillae located at the lid margin. C, Immunohistological analysis shows $CD20^+$ B lymphocyte clusters (green) and a surrounding $CD3^+$ marginal T lymphocyte zone (red). D, $CD35^+$ FDCs (red) are observed in a $CD20^+$ B lymphocyte cluster (green). Original magnification: C, ×200; D, ×400.

were in their adolescence without other atopic manifestations. We diagnosed VKC by histological methods in cases 1 and 2, and by clinical findings in case 3. We also found typical giant papillae on the upper tarsal conjunctiva in 2 patients (cases 1 and 3), and all 3 patients were well controlled by treatment with topical dexamethasone eye drops and tacrolimus eye drops. These findings were consistent with our diagnoses. The existence of eosinophils (Fig. 1A and see Figure, Supplemental Digital Content 3, http://links.lww.com/ICO/A164), and mast cells with surface IgE in the inferior tarsal giant papillae (see Figure, Supplemental Digital Content 4, http://links.lww.com/ICO/A164) were also in agreement with the pathological features of VKC.

Interestingly, the giant papillary formation occurred at the lid margin of the inferior tarsal conjunctiva in all 3 patients (Figs. 1, 2 and see Figure, Supplemental Digital Content 7, http://links.lww.com/ICO/A165). The anatomic location of the inferior tarsal giant papillae coincided with the location of conjunctiva-associated lymphoid tissue of the inferior tarsal conjunctiva, which is located at the lid margin of the inferior tarsal conjunctiva.[5] Interactions among antigens, antigen-presenting cells, and T lymphocytes/B lymphocytes occur in lymphoid tissue to achieve efficient immune responses.[6] It is known that ectopic lymphoid structures are induced at the site of inflammation during chronic inflammatory reactions and are termed a TLO.[7] We found TLO formation in the inferior giant papillae of case 1 (data not shown) and case 2 (Figs. 2C, D), characterized by CD20-positive B cell clusters with FDC, marginal zone T cells as in our previous study.[3] Thus, we considered that chronic allergic stimuli could induce TLO formation based on the conjunctiva-associated lymphoid tissue structure not only in the upper tarsal conjunctiva but also in the inferior tarsal conjunctivae.

In conclusion, we found giant papillae of VKC not only on the superior tarsal conjunctiva but also on the inferior tarsal conjunctiva, and the possibility of the presence of giant papillae on the inferior tarsal conjunctiva should be considered in the clinical examination of patients with VKC.

REFERENCES

1. Bonini S, Bonini S, Lambiase A, et al. Vernal keratoconjunctivitis revisited: a case series of 195 patients with long-term followup. *Ophthalmology.* 2000;107:1157–1163.
2. Barney N. Vernal and atopic keratoconjunctivitis. In: Krachmer J, ed. *Cornea.* St. Louis, Mosby; 2011:573–581.
3. Matsuda A, Ebihara N, Yokoi N, et al. Lymphoid neogenesis in the giant papillae of patients with chronic allergic conjunctivitis. *J Allergy Clin Immunol.* 2010;126:1310–1312.e1.
4. Matsuda A, Okayama Y, Ebihara N, et al. Hyperexpression of the high-affinity IgE receptor-beta chain in chronic allergic keratoconjunctivitis. *Invest Ophthalmol Vis Sci.* 2009;50:2871–2877.
5. Knop N, Knop E. Conjunctiva-associated lymphoid tissue in the human eye. *Invest Ophthalmol Vis Sci.* 2000;41:1270–1279.
6. Neyt K, Perros F, GeurtsvanKessel CH, et al. Tertiary lymphoid organs in infection and autoimmunity. *Trends Immunol.* 2012;33:297–305.
7. Aloisi F, Pujol-Borrell R. Lymphoid neogenesis in chronic inflammatory diseases. *Nat Rev Immunol.* 2006;6:205–217.

Three-Year Outcome of Descemet Stripping Automated Endothelial Keratoplasty for Bullous Keratopathy After Argon Laser Iridotomy

Satoru Nakatani, MD, PhD, and Akira Murakami, MD, PhD

Purpose: The aim of this study was to evaluate the 3-year outcome of Descemet stripping automated endothelial keratoplasty (DSAEK) for the treatment of bullous keratopathy secondary to argon laser iridotomy (ALI).

Methods: A total of 22 consecutive patients (22 eyes) with ALI who underwent DSAEK were retrospectively analyzed. Best spectacle-corrected visual acuity (BSCVA), endothelial cell density, and complications were investigated over 3 years postoperatively. The outcome of DSAEK was also compared between the ALI group and 21 other patients with Fuchs endothelial dystrophy (FED) or pseudophakic bullous keratopathy (PBK) (FED/PBK group).

Results: The median BSCVA improved from logarithm of the minimum angle of resolution 1.40 before DSAEK to 0.30 at 6 months, 0.30 at 12 months, 0.22 at 24 months, and 0.15 at 36 months after surgery. The median endothelial cell loss was 20.3% at 6 months, 18.4% at 12 months, 32.5% at 24 months, and 46.5% at 36 months. Comparison of the ALI group with the FED/PBK group showed no significant difference in the BSCVA or endothelial cell density. Rejection affected 9.1% of the ALI group versus 0% of the FED/PBK group ($P = 0.49$), the graft dislocation rate was 0% versus 9.5% ($P = 0.23$), and posterior synechiae were found in 31.8% versus 4.8% ($P = 0.046$).

Conclusions: The 3-year outcome of DSAEK for bullous keratopathy after ALI was excellent. However, caution should be exercised in patients with a history of ALI to avoid posterior synechiae after DSAEK.

Key Words: Descemet stripping automated endothelial keratoplasty, bullous keratopathy, argon laser iridotomy, endothelial cell density, posterior synechia, shallow anterior chamber

(*Cornea* 2014;33:780–784)

Received for publication March 2, 2014; revision received April 11, 2014; accepted April 13, 2014. Published online ahead of print June 9, 2014.
From the Department of Ophthalmology, Juntendo University Graduate School of Medicine, Tokyo, Japan.
The authors have no funding or conflicts of interest to disclose.
This study was approved by the Ethical Committee of the Juntendo University Graduate School of Medical Science and followed the tenets of the Declaration of Helsinki.
Reprints: Satoru Nakatani, MD, PhD, Department of Ophthalmology, Juntendo University Graduate School of Medicine, 3-1-3 Hongo Bunkyo-ku, Tokyo 113-8431, Japan (e-mail: satoru-n@juntendo.ac.jp).

Bullous keratopathy (BK) can be caused by many factors, and it is often an indication for Descemet stripping automated endothelial keratoplasty (DSAEK). In Japan, argon laser iridotomy (ALI) is one of the typical factors that predisposes patients to BK; ALI is the second highest cause of BK,[1] and such patients are expected to increase in the future.[2] Although several theories have been advanced concerning the mechanism underlying the induction of BK by ALI,[3–8] it has not been fully elucidated. No reports have been published concerning the long-term changes of endothelial cell density (ECD) after DSAEK for BK secondary to ALI. Accordingly, we investigated the 3-year outcome of DSAEK for ALI-induced BK, which is reported here together with a discussion of the appropriateness and limitations of this procedure.

MATERIALS AND METHODS

We retrospectively reviewed patients who underwent DSAEK for BK secondary to ALI at the Juntendo University Hospital between January 2008 and December 2010. Twenty-two consecutive patients (22 eyes) were followed up postoperatively for at least 3 years. DSAEK was performed by the same surgeon in all 22 patients. Their clinical records were reviewed to extract demographic characteristics, details of surgery, and intraoperative and postoperative complications. In addition, best spectacle-corrected visual acuity (BSCVA) and ECD were investigated preoperatively; at 6 months postoperatively; and at 1, 2, and 3 years postoperatively. The outcome of DSAEK was compared between these 22 patients (the ALI group) and 21 other patients with Fuchs endothelial dystrophy (8 eyes) or pseudophakic BK (13 eyes) (FED/PBK group) who also underwent DSAEK during the same period at our hospital. All measurements of visual acuity and corneal ECD were performed by skilled technicians at our hospital. Decimal visual acuity was measured and then converted to the logarithm of the minimum angle of resolution (logMAR). Postoperatively, the ECD of each patient was measured repeatedly at the central cornea by using a noncontact specular microscope (Konan Medical Corporation, Hyogo, Japan), and the most reliable data were used. Measurement was performed automatically but was also done manually if automated measurement was found to be difficult. The anterior eye segment was examined by slit-lamp biomicroscopy, optical coherence tomography (OCT), and by using the Pentacam (Oculus, Inc, Wetzlar, Germany). The

depth of the anterior chamber and the diameter of the recipient cornea were determined by the repeated measurement with OCT and the Pentacam.

Our study followed the principles of the Declaration of Helsinki. Approval of the protocol was obtained from the Research Ethics Board of Juntendo University (Tokyo, Japan), and the patients gave written informed consent to undergo each surgical procedure.

Surgical Technique

DSAEK was performed under sub-Tenon anesthesia with 1% xylocaine. In all phakic eyes, ultrasonic phacoemulsification/aspiration and intraocular lens (IOL) implantation were performed simultaneously. In eyes with poor anterior chamber visibility resulting from severe edema secondary to BK, after scraping off the corneal epithelium, visibility was improved by staining the anterior capsule with indocyanine green or by intracameral lighting with a light guide for vitreous surgery before cataract surgery was performed. In all patients, inferior peripheral iridectomy was performed using a 25-G vitreous cutter. As much as possible, Descemet membrane of the recipient was stripped off from the posterior corneal stroma over a region corresponding to the dimensions of the graft. In all patients, the surgeon used artificial anterior chambers and a Moria ALTK microkeratome (ALTK CBm; Moria) with a 300-μm head to prepare corneal grafts from corneas supplied by the Juntendo Eye Bank. After the graft was inserted into the anterior chamber by the pull-in method with a Busin glide (Asico, Westmont, IL), the corneal layer was closed with 2 or 3 10-0 nylon sutures. The anterior chamber was filled with air, and then the position of the graft was adjusted so that it was at the center of the cornea. After drainage through the corneal puncture site, the patient rested in a supine position for approximately 10 minutes on the operating table. On completion of the surgery, there was sometimes enough air in the anterior chamber to cover the entire cornea. However, it was adjusted so that the intraocular pressure was approximately 20 mm Hg, and the anterior chamber did not become too deep.

Postoperative Care

In general, the air was left to diffuse spontaneously out of the anterior chamber while the patient rested in the supine or sitting position, but air was partially eliminated through a corneal wound in some patients to alleviate pupillary block. To prevent postoperative posterior synechiae, tropicamide was applied topically 4 times a day for approximately 2 weeks. Topical levofloxacin hydrate and betamethasone sodium were initiated at 4 times a day and gradually decreased, whereas topical application of 0.1% fluorometholone was maintained. From the day of the surgery, administration of oral prednisolone (1 mg/kg) was tapered gradually and was discontinued after approximately 2 weeks. Because famotidine was administered orally to prevent gastric ulcer, there were no adverse reactions to steroids that required additional treatment.

Statistical Analysis

The data on ECD and BSCVA did not show a normal distribution, so the median and interquartile range are reported, and comparisons were performed by using the Wilcoxon rank sum test. Proportional demographic data were compared using χ^2 analysis. All reported P values are 2-sided, and $P < 0.05$ was considered to indicate statistical significance. Statistical analyses were performed with Stata/IC12.0 for Windows (Stata Corp LP, TX).

RESULTS

The mean age of the patients in the ALI group at the time of DSAEK was 75.4 ± 5.4 years (range: 60–86 years), and 77.2% of them were women. The mean interval from ALI to DSAEK was 6.9 ± 4.0 years (range: 2–15 years). The mean period from the onset of corneal endothelial dysfunction to DSAEK was 15.3 ± 15.9 months (range: 5–72 months). Onset of corneal endothelial dysfunction was defined as the occurrence of persistent corneal epithelial or parenchymal edema resulting from corneal endothelial cell loss. ALI was performed for glaucoma attacks in 8 eyes (36.4%), whereas it was performed to prevent glaucoma resulting from a shallow anterior chamber in the other 14 eyes (63.6%). At the time of DSAEK, 7 eyes (31.8%) were pseudophakic. The phakic eyes were treated by combined ultrasonic emulsification/aspiration and IOL implantation. None of the patients in the ALI group had a history of filtering surgery, whereas 5 patients in the FED/PBK groups did have a history of this surgery. Glaucoma was being treated with ophthalmic solutions in 5 eyes (22.7%). Fuchs corneal endothelial dystrophy–like findings associated with guttae in the contralateral eye were confirmed in 4 eyes (18.2%). One patient had diabetes, but glycemic control was adequate with oral therapy, and diabetic retinopathy was not noted. Because 90.9% of the patients were referred from other hospitals, the laser irradiation conditions at the time of ALI were only known for 3 of them and the laser dose was ≤5 J in all 3 patients. Table 1 compares the demographic characteristics and other factors between the ALI and FED/PBK groups.

There were no intraoperative complications, such as iris prolapse, observed during graft insertion or posterior capsular breakage during cataract surgery. Postoperative graft dislocation and reinjection of air did not occur. Pupillary block was observed on the day of surgery in 3 eyes (13.6%), but this improved in all cases on the same day owing to mydriasis, maintenance of a sitting position, and elimination of air through a corneal incision. Posterior synechiae that obviously affected the light reflex were noted in 7 eyes (31.8%) at 3 years postoperatively. Synechiae were present before DSAEK in 2 of these eyes, whereas synechiae occurred after DSAEK in the other 5 eyes. Slit-lamp microscopy revealed few cells and little flare in the anterior chamber of all the patients. All the posterior synechiae were partial, and there were no patients with serious lesions such as circumferential synechiae. In this study, synechiae were classified as present if detected by slit-lamp microscopy, and a detailed investigation using OCT or other methods was not performed. Ocular

TABLE 1. Demographic Profile and Surgical Parameters

	ALI Group (n = 22)	FED/PBK Group (n = 8) (n = 13)	*P*
Age (yrs), mean (SD)	75.4 (5.4)	75.0 (8.6)	0.86
Gender (female) (%)	17 (77.3)	9 (42.9)	0.046
Duration of BK before DSAEK (mos), mean (SD)	15.3 (15.9)	13.8 (12.5)	0.72
Donor age (yrs), mean (SD)	67.4 (17.9)	67.3 (18.1)	0.99
Preexisting glaucoma (%)	5 (22.7)	6 (28.6)	0.93
Preoperative synechiae (%)	2 (9.1)	1 (4.8)	0.91
Anterior chamber depth, phakic eye (mm) (n)	1.5 (15)	2.6 (8)	<0.01
Pseudophakic eye (mm) (n)	3.3 (7)	3.4 (13)	0.36
Recipient cornea diameter (mm), mean (SD)	10.8 (0.4)	10.9 (0.6)	0.58
Graft diameter (mm), mean (SD)	8.1 (0.3)	8.2 (0.4)	0.20
Simultaneous cataract surgery (%)	15 (68.2)	8 (38.1)	0.095
Descemet membrane peeling (%)	16 (72.7)	12 (57.1)	0.45

P values: *t* test for unpaired samples or χ^2 test.

hypertension required postoperative treatment with ophthalmic solutions for glaucoma in 4 eyes (18.2%). Three of these 4 eyes had received topical glaucoma therapy before DSAEK. Rejection occurred in 2 eyes (9.1%). It was controlled by oral steroid therapy in 1 eye, but graft failure that required repeat DSAEK occurred in the other eye. Table 2 shows a comparison of complications and other factors between the ALI and FED/PBK groups.

The median BSCVA was logMAR 1.40 preoperatively, whereas it was logMAR 0.30, 0.30, 0.22, and 0.15 at 6, 12, 24, and 36 months after surgery, respectively. There were no significant differences at any time between the ALI and FED/PBK groups (Table 3). The median preoperative donor corneal ECD was 2832 cells per square millimeter (interquartile range: 2620–2906 cells per square millimeter), and the median postoperative decrease of ECD was 20.3%, 18.4%, 32.5%, and 46.5% after 6, 12, 24, and 36 months, respectively. These parameters showed no significant differences between the ALI and FED/BPK groups at any time (Table 4).

DISCUSSION

The mechanism of endothelial cell loss after ALI has not been elucidated, and the rate of ECD decline after this procedure has not been clarified fully. Shimazaki et al[1] and Ang et al[2] reported that the mean interval from ALI to corneal transplantation was 6.8 and 6.9 years, respectively. In the present series, the mean period until the performance of DSAEK was 6 years and 10 months. Because this period included the waiting time for corneal transplantation, the actual interval from the ALI until the onset of corneal endothelial dysfunction was slightly shorter, and was 5 years and 7 months (range: 12–174 months). The 3-year outcome of DSAEK for BK secondary to ALI was similar to that of DSAEK for FED or PBK, and the rate of ECD decline after the ALI was almost identical to that previously reported in studies on the long-term outcome of DSAEK.[9,10] In the present series, corneal endothelial dysfunction was noted from <6 years after ALI, but the rate of endothelial cell loss during the 3-year period after DSAEK was similar to that in other diseases.

It has been reported that it can be difficult to perform DSAEK or combined cataract surgery in Japanese patients with BK secondary to ALI because of a shallow anterior chamber and poor intracameral visibility.[11–13] In the present series, however, there were no severe intraoperative or postoperative complications, and favorable results were obtained. This was presumably because adequate visibility to perform cataract surgery was obtained by anterior capsular staining and intracameral lighting before commencing this surgery. Even when the anterior chamber was shallow, the graft could be positioned as usual by using a Busin glide. In the eyes with a shallow anterior chamber, the graft was temporarily folded after insertion, but it was not so difficult to spread it out because the corneal stroma has the ability to return spontaneously to its original shape. Iris prolapse during graft insertion can be prevented if the incision is prepared carefully and the perfusion pressure is not increased unnecessarily. Even if prolapse occurs, it can be dealt with by taking appropriate measures during graft insertion.[12] The ciliary zonule was weak in some patients from the present series, but intracapsular IOL fixation could be achieved by carefully performing cataract surgery. Even if ciliary zonular rupture occurs, surgery can be continued if the IOL is sutured to the ciliary sulcus. Thus, if DSAEK is performed after making adequate

TABLE 2. Complications and Adverse Events

	ALI Group (n = 22)		FED/PBK Group (n = 8) (n = 13)		
	No.	%	No.	%	*P*
Graft detachment	0	0	2	9.5	0.23
Graft rejection	2	9.1	0	0	0.49
Primary failure	0	0	3	14.3	0.11
Pupillary block immediately after DSAEK	3	13.6	4	19.0	0.70
Late IOP elevation	4	18.2	6	28.6	0.95
Posterior synechiae	7	31.8	1	4.8	0.046

P values: χ^2 test.
IOP, intraocular pressure.

TABLE 3. Average BSCVA Before and After DSAEK

	ALI Group (n = 21)	FED/PBK Group (n = 7) (n = 11)	
	Median logMAR (Interquartile Range)	Median logMAR (Interquartile Range)	*P*
Before surgery	1.40 (1.20–1.70)	1.26 (1.00–2.00)	0.94
6 mos	0.30 (0.22–0.52)	0.30 (0.17–0.52)	0.88
1 yr	0.30 (0.046–0.40)	0.40 (0.15–0.40)	0.64
2 yrs	0.22 (0.046–0.40)	0.26 (0.17–0.47)	0.83
3 yrs	0.15 (0.046–0.52)	0.30 (0.22–0.66)	0.29

P values: Wilcoxon rank sum test.

preparations by considering the characteristics of eyes with a shallow anterior chamber, most intraoperative complications can be prevented and effective countermeasures can be taken if any complications occur. In fact, a shallow and small anterior chamber has some advantages for performing DSAEK. In eyes with a shallow anterior chamber and a small cornea diameter, the volume of air injected can be reduced and the graft can be positioned more stably. Furthermore, attachment of grafts could be achieved with a small volume of air, and little adjustment of the position was needed. In the present series, DSAEK was performed after making adequate preparations based on the characteristics of eyes with a shallow anterior chamber, so there were no intraoperative complications, such as posterior capsular breakage or iris prolapse, and postoperative graft dislocation was not seen either.

The visual acuity of the ALI group was approximately 20/40 at 3 years after DSAEK. Compared with the mean visual acuity of 20/25 at 3 years postoperatively that was recently reported,[14] the present results were slightly worse. However, there was no significant difference of postoperative visual acuity between the ALI group and the FED/PBK group in this study. This suggests that a relatively poor postoperative visual acuity is a problem common to all patients undergoing DSAEK at our hospital, presumably because many of our patients have poor visual acuity before the procedure. The mean visual acuity before DSAEK was 20/51 in the above-mentioned report,[14] whereas it was 20/540 in this study. Further, DSAEK was performed at >1 year after the onset of endothelial dysfunction in the majority of our patients, suggesting that irreversible parenchymal opacity had already occurred in many cases, which was likely to inhibit the postoperative improvement of visual acuity. If endothelial dysfunction occurs after ALI, DSAEK should be performed as soon as possible. However, further investigations are required to confirm this point, because the Japan Eye Bank does not have an adequate supply of donor corneas.

In this series, postoperative complications of posterior synechiae and pupillary block occurred in 7 (31.8%) and 3 eyes (13.6%), respectively. It is possible that these complications were related to excess air on the completion of surgery. However, it seems that posterior synechiae tend to occur after DSAEK for ALI, because the incidence of this complication was significantly lower in the FED/PBK group (4.8% or 1 eye, $P = 0.046$), in which DSAEK was performed under the same conditions as in the ALI group (Table 2). It could also be suggested that posterior synechiae tended to occur because of a shallow anterior chamber itself, but this possibility could be excluded because the depth of the anterior chamber showed no appreciable difference between the eyes in the ALI group undergoing cataract surgery and the eyes in the FED/PBK group (Table 1). Because Japanese studies have shown that anterior chamber inflammation tends to occur after penetrating corneal transplantation in post-ALI eyes, posterior synechiae were also considered to result from postoperative inflammation after DSAEK. However, the incidence of pupillary block was

TABLE 4. Endothelial Cell Loss After DSAEK

	ALI Group (n = 21)	FED/PBK Group (n = 7) (n = 11)	
	Median (Interquartile Range)	Median (Interquartile Range)	*P*
ECD (cells/mm^2)			
Baseline	2832 (2620–2906)	2849 (2668–3030)	0.91
Endothelial cell loss (%)			
6 mos	20.3 (10.6–23.9)	12.3 (9.3–25.7)	0.66
1 yr	18.4 (13.7–41.1)	14.6 (10.3–22.9)	0.22
2 yrs	32.5 (13.6–55.4)	22.3 (11.8–39.5)	0.78
3 yrs	46.5 (16.2–64.35)	45.1 (23.2–64.0)	0.83

P values: Wilcoxon rank sum test.

higher in the FED/PBK group (4 eyes or 19.0%, $P = 0.70$), presumably because of a relatively large amount of residual air present when using our surgical technique. However, this posed no serious problems because we took appropriate corrective measures early after surgery. Reducing the volume of air in the anterior chamber on the completion of surgery would be effective for prevention of such complications, but is associated with the potential risk of postoperative graft dislocation. The results of this study were obtained in patients receiving both topical and oral steroid therapy, suggesting that adequate control of inflammation is essential in any case. The mean ECD loss at 3 years postoperatively was 54.7% for patients with posterior synechiae. Although there was no significant difference between the patients with and without synechiae ($P = 0.22$), ECD loss was still higher than the overall mean in patients with posterior synechiae. Therefore, attention should be paid to this point in the future.

The limitations of this study were a small sample size and relatively short follow-up period. Because different results might be obtained if the number of patients is increased and the observation period is prolonged, a long-term study in a larger patient population is required.

In conclusion, although it is necessary to pay attention to postoperative posterior synechiae, DSAEK is an effective surgical technique for the treatment of BK secondary to ALI because the 3-year outcome is comparable with that of DSAEK for treatment of FED/PBK. It was also confirmed that DSAEK should be performed by paying careful attention to several points in eyes with a shallow anterior chamber and that satisfactory results can be obtained if surgery is commenced after making adequate preparations based on consideration of such issues.

REFERENCES

1. Shimazaki J, Amano S, Uno T, et al. National survey on bullous keratopathy in Japan. *Cornea*. 2007;26:274–278.
2. Ang LP, Higashihara H, Sotozono C, et al. Argon laser iridotomy-induced bullous keratopathy—a growing problem in Japan. *Br J Ophthalmol*. 2007;91:1613–1615.
3. Schwartz A, Martin NF, Weber PA. Corneal decompensation after argon laser iridotomy. *Arch Ophthalmol*. 1988;106:1572–1574.
4. Smith J, Whitted P. Corneal endothelial changes after argon laser iridotomy. *Am J Ophthalmol*. 1984;98:153–156.
5. Wilhelmus KR. Corneal edema following argon laser iridotomy. *Ophthalmic Surg*. 1992;23:533–537.
6. Kaji Y, Oshika T, Usui T, et al. Effect of shear stress on attachment of corneal endothelial cells in association with corneal endothelial cell loss after laser iridotomy. *Cornea*. 2005;24(suppl 1):S55–S58.
7. Lim LS, Ho CL, Ang LP, et al. Inferior corneal decompensation following laser peripheral iridotomy in the superior iris. *Am J Ophthalmol*. 2006;142:166–168.
8. Yamamoto Y, Uno T, Shisida K, et al. Demonstration of aqueous streaming through a laser iridotomy window against the corneal endothelium. *Arch Ophthalmol*. 2006;124:387–393.
9. Price MO, Fairchild KM, Price DA, et al. Descemet's stripping endothelial keratoplasty: five-year graft survival and endothelial cell loss. *Ophthalmology*. 2011;118:725–729.
10. Ratanasit A, Gorovoy MS. Long-term results of Descemet stripping automated endothelial keratoplasty. *Cornea*. 2011;30:1414–1418.
11. Hirayama M, Yamaguchi T, Satake Y, et al. Surgical outcome of Descemet's stripping automated endothelial keratoplasty for bullous keratopathy secondary to argon laser iridotomy. *Graefes Arch Clin Exp Ophthalmol*. 2012;250:1043–1050.
12. Kobayashi A, Yokogawa H, Sugiyama K. Descemet stripping with automated endothelial keratoplasty for bullous keratopathies secondary to argon laser iridotomy—preliminary results and usefulness of double-glide donor insertion technique. *Cornea*. 2008;27:62–69.
13. Kobayashi A, Yokogawa H, Sugiyama K. Non-Descemet stripping automated endothelial keratoplasty for endothelial dysfunction secondary to argon laser iridotomy. *Am J Ophthalmol*. 2008;146:543–549.
14. Li JY, Terry MA, Goshe J, et al. Three-year visual acuity outcomes after Descemet's stripping automated endothelial keratoplasty. *Ophthalmology*. 2012;119:1126–1129.